Development of H_2O_2 Triggered Ion Transporter

5th year MS thesis (August 2023)

By

Ronedy Naorem

(Roll No. 20191067)

Under the Guidance of

Prof. Pinaki Talukdar

Department of Chemistry

Indian Institute of Science Education and Research Pune

Dr. Homi Bhabha Road, Pashan, Pune

This page was left blank on purpose

Certificate

This is to certify that this dissertation entitled “Development of H_2O_2 triggered ion transporter” towards the partial fulfilment of the BS-MS dual degree programme at the Indian Institute of Science Education and Research, Pune represents study/work carried out by Ronedy Naorem at the Indian Institute of Science Education and Research (IISER), Pune under the supervision of Prof. Pinaki Talukdar, Department of chemistry IISER, Pune during the academic year 2023-2024.

Signature of Supervisor

Declaration

I hereby declare that the matter embodied in the report entitled "Development of H_2O_2 triggered ion transporter" are the results of the work carried out by me at the Department of Chemistry, Indian Institute of Science Education & Research (IISER) Pune, under the supervision of Prof. Pinaki Talukdar, and the same has not been submitted elsewhere for any other degree. Wherever others contribute, every effort is made to indicate this clearly, with due reference to the literature and acknowledgement of collaborative research and discussions.

Ronedy Naorem

20191067

Signature of student

Acknowledgements

On this journey of my MS thesis, I received a tremendous amount of help from numerous people; without their support, I could have never completed the work that I have done in this thesis. Hence, in this section, I would like to thank all those individuals for making my MS thesis complete and made a memorable part of my life.

I would like to express my thanks to my thesis supervisor, Prof. Pinaki Talukdar, for giving me the opportunity to work in his lab a year before starting my MS thesis. He provided me with the opportunity to work in his lab and introduced me to his group. I am grateful for his guidance, encouragement, and support throughout all my projects. I also thank him for supporting me get experience in biological studies as well.

I would like to thank Dr. Debangsu Sil (IISER, Pune) for accepting to be my expert for the MS-thesis work and for the valuable inputs during my Mid-term report.

For the Biological assays that are involved in the thesis, I thank Dr. Mayurika Lahiri for providing me with the lab in the biology department and for teaching me the cell culture work personally. I thank her again for all her valuable suggestions and support in the meetings.

I express my gratitude to my mentors, Naveen Joseph Roy and Dr. Manzoor Ahmed, for guiding me through the learning process in the lab. Umesh Shivpuje and Arjun Jagdish for helping me out in the areas I lack experience in and out of the lab. I thank Benchamin Abraham and Ajay Malik from ML lab for their constant support in my biological assays.

I have been blessed with a group of people who have supported me throughout the projects. Firstly, I thank Dr. Abhishek Mondal, Akram Raza, Dr. Avisikta Upadhyay, Dr. Debashis Mondal, Debarati Sadhukhan, Debraj Ganguly, Neelam Raturi, Pathan Shaharukh Khan, Payel Nandi, Dr. Rashmi Sharma, Ranjeet Patil, Sandip Chattopadhyay, Soumayajit Ghosh, Tanvi Vyas, Ahan Chatterjee, Arshad A, Anirban Mukherjee, Ankit Jagdand, Kavan Nandaniya and Shreya Das who are the past and present member of our lab for giving me all the supports and so many sweet memories in my project period. Secondly, I would like to thank Atharva Bhingare, Shreyas Nadiger, Soham Chandak, Abhijith Menon, Vaishak Bhat, Subramanya Gond, Prathith Bhargav, Abhinav Dhawan, Sanjay Bhandarkar, Shridhar Shanbhag and Tushar Gavali for their support outside the lab.

I sincerely thank the staff at IISER Pune, Nitin Dalvi (NMR), Sandeep Mishra (NMR), and Sandeep Kanade (HRMS) for their help in the characterization of my compounds.

I am thankful to my family for their unconditional love and support, without whom I would not be able to reach till this stage of life.

I acknowledge that this thesis work was an extension of my mentor Naveen’s thesis work on the Bis-salicylamide transporter, and some parts of the work are reproduced from his work.

Contents

1. Abstract

Ion transporters are known to induce apoptosis in the cancer cell and, hence, are a potential candidate for a cancer-curing drug. But unfortunately they have a downside of being unable to differentiate between cancer cells and normal human cells. One of the best ways to overcome this problem is to develop a stimuli-responsive ion transporter, which will enable the ion transporter to target the cancer cell specifically. Keeping in mind that the concentrations of reactive oxygen species like hydrogen peroxide are elevated in cancer tissue, we developed a phenyl boronic ester caged bis salicylamide ion transporter, which can be activated in the presence of higher concentrations of hydrogen peroxide.

2. Introduction:

In nature, ion transport has the function of cell proliferation, cell 9ignalling, osmotic regulation, Ionic homeostasis, etc. Because of these functions of ion transporters, any disruption of them can create a lot of problems. In humans, a group of diseases called channelopathies (e.g., Cystic Fibrosis, Bartter syndrome, Dravet syndrome, etc.) arises due to problems in the ion transporters of the body.[1] To combat such disease, the development of artificial ion transporter, which can replace the natural ones, is of great interest. But at the same time, if we think from a different angle, the presence of excess ion transporter can also disrupt the homeostasis of the cell and cause cell death in unwanted cells like cancer cells.

Synthetic small molecule ion transporters are of great interest in cancer research as it is known to induce apoptotic cell death in cancer cells via the disruption of their tightly controlled ion homeostasis.[2] At the same time, ion transporters have a severe limitation in their utility due to their non-specific activity towards healthy tissue.[3] Progress has been made to overcome the limitation of selectivity by linking labile moieties in the binding pocket of the transporter, which makes the system incapable of transporting the desired ions, creating a prodrug-transporter or 'protransporter'. This labile group can be cleaved off by using cancer tissue-specific stimuli (including upregulated metabolites)[4] and subsequently activate ion transport (Figure 1A).

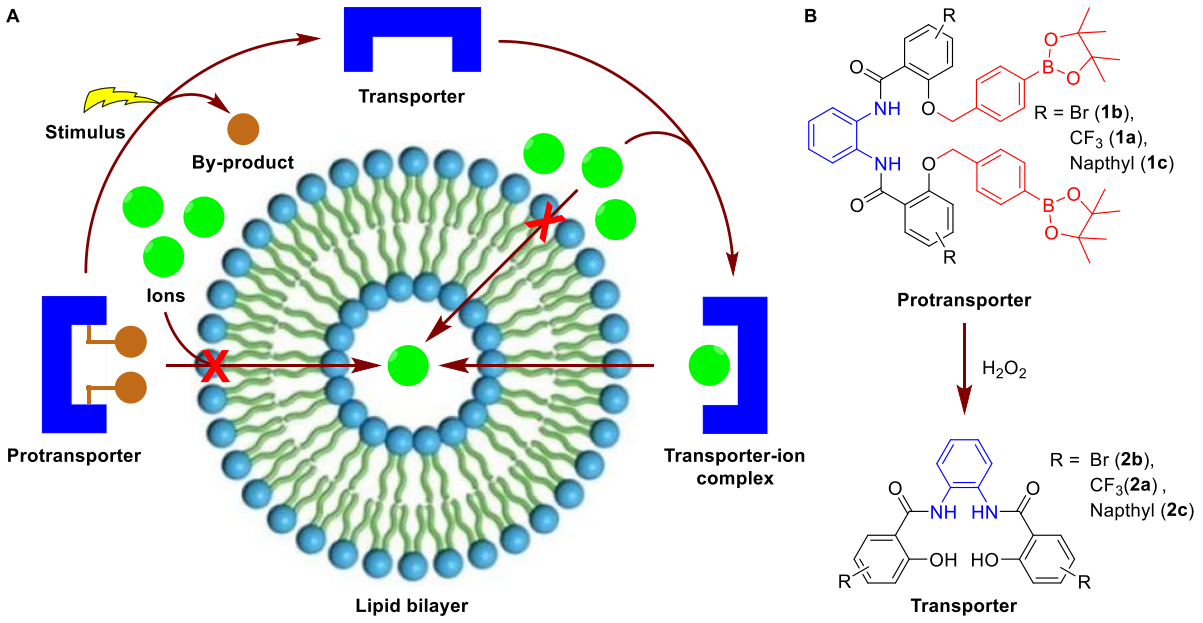

Figure 1. Illustration of stimuli-responsive activation of a protransporter for facilitating transmembrane ion transport (A). Structures of protransporters **1a-1c** and transporters **2a-2c** (B). The lipid bilayer model was adapted from reference 13.

Compared to healthy tissue, cancer tissues are inherently known to have high levels of reactive oxygen species (ROS) such as hydrogen peroxide[5] that contribute to their proliferation and DNA alteration,[6] which could be utilized as a stimulus for targeted prodrug activation. Phenylboronic esters are well known in the literature as H_2O_2 activable groups and have been used for a variety of applications such as fluorescent probes or for drug release.[7] Inspired by this idea, we propose the use of a phenyl boronic ester caged bissalicylamide ion transporter capable of being activated by H_2O_2 in cells (Figure1B). The reported mechanism for the activation of phenyl boroester in the presence of H_2O_2 is as follow (see **Figure 2**).

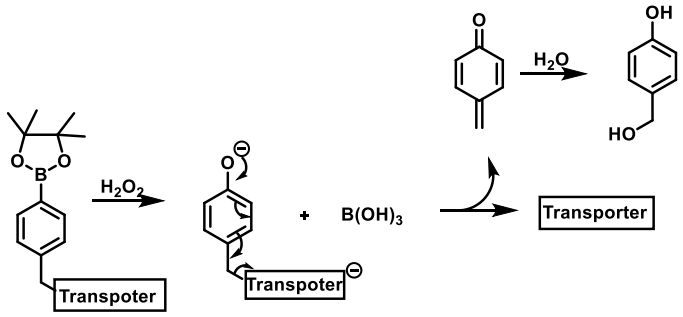

Figure 2: Reported mechanism of phenyl boroester activation with H_2O_2.[8]

The objective of this project is to: (1) synthesis and characterization of three derivatives of H_2O_2 activable protransporter and transporter systems; (2) characterization of H_2O_2-based activation of protransporters and transporters using HRMS, NMR, UV-Vis methods; (3) comparison of ion transport activities of protransporter and transporter systems across lipid vesicles, and the mechanism of ion transport by one of the synthesized transporter derivatives; (4) study of ion transport upon activation of protransporter by H_2O_2; and (5) verification of protransporters activation in cancer cells.

3. General Methods

3.1 Materials used

For the synthesis and purification of the all the compounds in this thesis work the reagents and solvents were purchased from commercial source (Sigma, Avra, TCI, BLD pharm, Spectrochem, Rankem, SRL) and were directly used without any further purification. For all column chromatography purification silica gel of mash size 230-400 from Spectrochem was used. Thin layer chromatography was done using Merck silica gel 60 F_{254} plates. Egg yolk phosphatidylcholine (EYPC) as a solution in chloroform (25 mg/mL), mini extruder set, and polycarbonate membrane of pore size

200 nm for vesicle preparation was purchased from Avanti Polar Lipids (Merck). Lucigenin, Sodium Nitrate, Triton X-100 and Sodium Chloride for the fluorescence studies were purchased from Sigma-Aldrich (Merck). All the stock solutions for all the studies were prepared in Milli-Q water or HPLC grade acetone or DMSO. The purifications using HPLC were performed on a CombiFlash EZprep preparative HPLC from TELEDYNE ISCO fitted with a C-18 reverse phase column.

3.2 Physical measurement

All the NMR spectra were taken using Bruker Avance III HD 400 MHz NMR spectrometer. Measurement for ^{1}H NMR, ^{13}C NMR and ^{19}F NMR were done in 400 MHz, 101 MHz and 377MHz respectively. The NMR spectra were calibrated using the residual peaks of the solvents. For the ^{19}F NMR trifluoroacetic acid was used as the reference peak (at δ = 75.75 ppm). The abbreviations used in the NMR data are: δ = chemical shift in ppm, *J* = coupling constant in Hz, s = singlet, d = doublet, t = triplet, q = quartet, m = multiplet, dd = doublet of doublet, dt = doublet of triplet, ddd= doublet of doublet of doublet. Infra-red spectra were recorded using Bruker ALPHA-E FT-IR spectrometry and reported in $\tilde{\nu}$ $(cm)^{-1}$. Mass spectrometry was done in matrix assisted laser desorption/ionization (MALDI) and high resolution mass spectrometry (HRMS). MALDI was recording using AB SCIEX TOF/TOF^{TM} 5800 and HRMS was recorded on waters SYNAPT G2 mass spectrometer equipped with Waters Z-Spray^{TM} electrospray ionization (ESI) source. Fluorescence studies were performed in HORIBA Jobin Yvon Fluormax + spectrometer.

All the NMR data were process using MestReNova software. The fluorescence studies were processed using OriginPro 8.5 and MS Excel software. The figures and the chemical structures were drawn using ChemDraw 21.0.0.

3.3 Synthesis

i. Retro synthesis

The following is the synthetic route that we planned to follow for the preparation of the protransporter and the transporter.

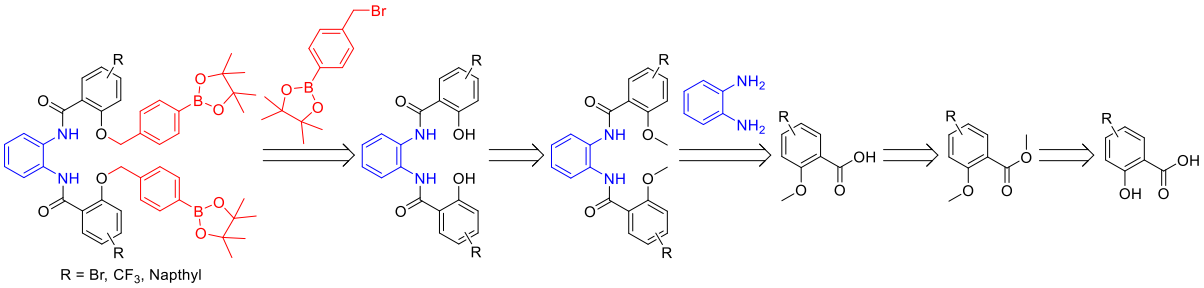

Scheme 1: Proposed synthetic route for the preparation of H_2O_2-responsive protransporter.

ii. Complete synthesis and characterization

Following **Scheme 1** we were able to synthesize all the intended compounds. **Scheme 2** describes the synthetic steps, yields of the reactions and the numbering of the compounds (the corresponding numberings will be used to refer the compound).

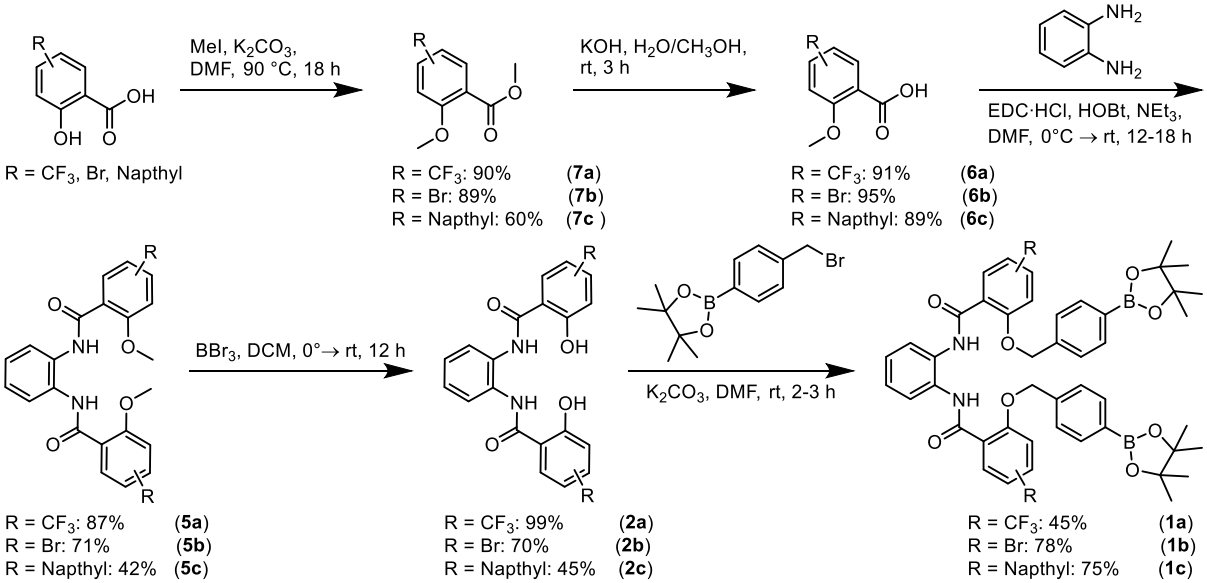

Scheme 2: Synthesis and yields of designed transporters and protransporters.

Synthesis of substituted methyl 2-methoxybenzoates:

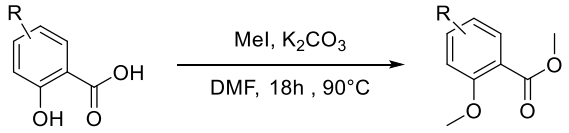

General Procedure A: To a stirred suspension of the substituted salicylic acid (1 eq.) and K_2CO_3 (2.5 eq.) in DMF (1 mL per 100 mg substituted salicylic acid) was added Iodomethane (2.42 eq.) and stirred for 18 h at 90 °C. It was then diluted with EtOAc and washed with water. The aqueous layer was further extracted with EtOAc (3 times). The entire acquired organic layer was combined and a brine wash was given. This organic layer was dried using anhydrous Na_2SO_4 and solvent was evaporated in rota vapour to obtain our desired compound.

methyl 4-bromo-2-methoxybenzoate (7b)

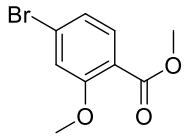

Physical appearance: Orange oil (liquid); Yield = 89%; **^{1}H NMR (400 MHz, $CDCl_3$)**: δ 7.69 – 7.66 (m, 1H), 7.12 (dt, *J* = 4.0, 1.8 Hz, 2H), 3.90 (s, 3H), 3.87 (s, 3H); **^{13}C NMR (101 MHz, $CDCl_3$)**: δ 166.05, 159.82, 133.04, 127.86, 123.54, 118.97, 115.80, 56.43, 52.27; **IR (ṽ cm^{-1})**: 2949.76, 1728.42, 1588.24, 1485.22, 1461.76, 1434.19, 1394.94, 1287.08, 1240.55, 1089.20, 1023.10, 858.22, 722.31; **HRMS (ESI)**: m/z $[M\text{-}OCH_3]^+$ Calc. for $C_9H_9BrO_3$: 212.9551, Found: 212.9546.

methyl 2-methoxy-4-(trifluoromethyl)benzoate (7a)

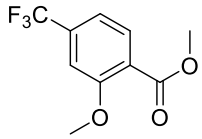

Physical appearance: Yellow oil; Yield = 85%; **^{1}H NMR (400 MHz, $CDCl_3$)**: δ 7.86 (d, *J* = 7.9 Hz, 1H), 7.24 (d, *J* = 8.0 Hz, 1H), 7.18 (s, 1H), 3.95 (s, 3H), 3.91 (s, 3H); **^{13}C NMR (101 MHz, $CDCl_3$)**: δ 165.91, 159.11, 135.05 (q, *J* = 65.3, 32.6 Hz), 132.16, 123.63, 123.56 (q, *J* = 272.8 Hz), 117.00 (q, *J* = 3.8 Hz), 108.99 (q, *J* = 3.7 Hz), 56.40, 52.53; **^{19}F NMR (377 MHz, $CDCl_3$)**: δ - 63.22; **IR (ṽ cm^{-1})**: 2954.76, 1734.16, 1412.43, 1328.45, 1240.43, 1170.58, 1124.77, 1092.60, 964.37, 892.20, 861.63, 742.08**;** **HRMS (ESI)**: m/z $[M+H]^+$ Calc. for $C_{10}H_9F_3O_3$: 235.0582, Found: 235.0575.

methyl 3-methoxy-2-naphthoate (7c)

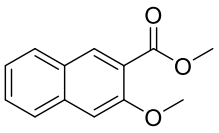

The residue was purified by silica gel column chromatography. **Eluent for column chromatography**: 8% EtOAc in petroleum ether; **Physical appearance**: Yellow oil(liquid); Yield = 55%; **^{1}H NMR (400 MHz, $CDCl_3$)**: δ 8.30 (s, 1H), 7.82 (d, *J* = 8.2 Hz, 1H), 7.74 (d, *J* = 8.2 Hz, 1H), 7.52 (ddd, *J* = 8.2, 6.9, 1.2 Hz, 1H), 7.38 (ddd, *J* = 8.1, 6.9, 1.1 Hz, 1H), 7.21 (s, 1H), 4.00 (s, 3H), 3.96 (s, 3H); **^{13}C NMR (101 MHz, $CDCl_3$)**: δ 166.84, 155.83, 136.23, 132.96, 128.83, 128.57, 127.63, 126.58, 124.53, 121.77, 106.89, 56.12, 52.43; **IR ($\tilde{\nu}$ cm^{-1})**: 2950.54, 1725.42, 1630.16, 1503.45, 1467.13, 1359.30, 1335.14, 1207.82, 1131.44, 1013.83, 954.10, 783.40, 746.22, 714.39; **HRMS (ESI)**: m/z $[M\text{-}OCH_3]^+$ Calc. for $C_{13}H_{12}O_3$: 185.0603, Found: 185.0601.

Synthesis of substituted 2-methoxybenzoic acids through hydrolysis

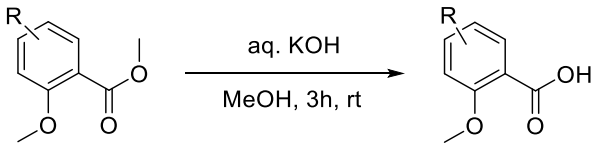

General Procedure B: To a solution of the ester in MeOH (2.7 mL per 100 mg ester) was added 6N aqueous KOH (26.5 eq.) and stirred for 3 h at rt. MeOH was then removed *in vacuo*. The mixture was quenched by addition of water (10 mL) followed by conc. HCl until pH ~ 2. It was then diluted with EtOAc and then washed with water. The aqueous layer was extracted exhaustively with EtOAc, the organic layers combined, washed with brine, dried over anhydrous Na_2SO_4, and the solvent removed *in vacuo*.

4-bromo-2-methoxybenzoic acid (6b)

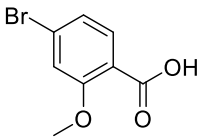

Physical appearance: yellowish white powder; Yield = 95%; **^{1}H NMR (400 MHz, $CDCl_3$)**: δ 8.02 (d, *J* = 8.4 Hz, 1H), 7.28 (dd, *J* = 8.4, 1.7 Hz, 1H), 7.22 (d, *J* = 1.7 Hz, 1H), 4.07 (s, 3H); **^{13}C NMR (101 MHz, $CDCl_3$)**: δ 165.34, 158.58, 134.94, 129.48, 125.59, 116.84, 115.61, 57.18; **IR ($\tilde{\nu}$ cm^{-1})**: 2946.53, 2813.29, 1681.51, 1588.03, 1562.44, 1295.15, 1237.54, 1015.65, 858.50, 828.91, 771.59; **HRMS (ESI)**: m/z $[M\text{-}OH]^+$ Calc. for $C_8H_7BrO_3$: 212.9551, Found: 212.9546.

2- methoxy-4-(trifluoromethyl)benzoic acid (6a)

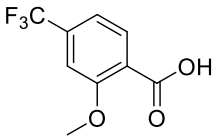

Physical appearance: white powder; Yield = 91%; **^{1}H NMR (400 MHz, $CDCl_3$)**: δ 8.28 (d, *J* = 8.1 Hz, 1H), 7.40 (dd, *J* = 8.1, 0.7 Hz, 1H), 7.28 (s, 1H), 4.14 (s, 3H); **^{13}C NMR (101 MHz, $CDCl_3$):** 165.44, 158.52, 136.51 (q, *J* = 33.1 Hz), 134.50, 123.22 (q, *J* = 2.7 Hz), 121.11 (d, *J* = 0.9 Hz), 118.61 (q, *J* = 0.0 Hz), 109.05 (q, *J* = 7.6, 3.8 Hz), 57.14; **^{19}F NMR (377 MHz, $CDCl_3$)**: δ - 63.32; **IR (ṽ cm^{-1})**: 2981.40, 1690.37, 1327.32, 1303.35, 1148.06, 1100.26, 1077.03, 1022.40, 898.48, 788.75; **HRMS (ESI)**: m/z $[M+H]^+$ Calc. for $C_9H_7F_3O_3$: 221.0426, Found: 221.0413.

3-methoxy-2-naphthoic acid (6c)

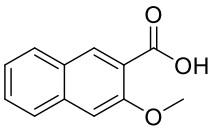

Physical appearance: white powder; Yield = 89%; **^{1}H NMR (400 MHz, $CDCl_3$)**: δ 10.94 (s, 1H), 8.79 (s, 1H), 7.91 (d, *J* = 8.1 Hz, 1H), 7.78 (d, *J* = 8.2 Hz, 1H), 7.59 (t, *J* = 7.5 Hz, 1H), 7.46 (t, *J* = 7.5 Hz, 1H), 7.31 (s, 1H), 4.18 (s, 3H); **^{13}C NMR (101 MHz, $CDCl_3$)**: δ 165.57, 154.41, 136.70, 136.41, 129.64, 129.59, 128.50, 126.67, 125.55, 118.01, 107.28, 56.81; **IR (ṽ cm^{-1})**: 2965.16, 2659.78, 1693.86, 1674.79, 1626.66, 1459.22, 1283.49, 1254.48, 1219.13, 1193.13, 1070.23, 865.44, 749.42**; HRMS (ESI)**: m/z $[M-OH]^+$ Calc. for:$C_{12}H_{10}O_3$: 185.0603, Found: 185.0595.

Synthesis of *o*-methylated bissalicylamides through acid-amine coupling

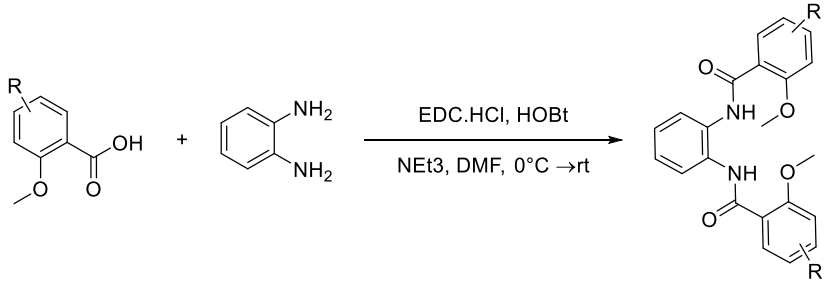

General Procedure C: To a solution of the substituted 2-methoxybenzoic acid (2.2 eq.) in DMF (6 mL per 100 mg *o*-phenylenediamine) was added *o*-phenylenediamine (1 eq.) followed by Et_3N (3 eq.) and cooled to 0 °C in an ice bath. Then HOBt (2.6 eq.) was added and the mixture stirred at 0 °C for 10 min. Finally, EDC·HCl (2.6 eq.) was added and the mixture stirred at 0 °C for 10 min. The mixture was then allowed to reach rt and stirred overnight for 24 h. It was then diluted with EtOAc and washed with water. The aqueous layer was further extracted with EtOAc (3 times),

the organic layers combined, washed with brine, dried over anhydrous Na_2SO_4, and the solvent removed *in vacuo*. The residue was purified by silica gel column chromatography.

***N*,*N*'-(1,2-phenylene)bis(4-bromo-2-methoxybenzamide)(5b)**

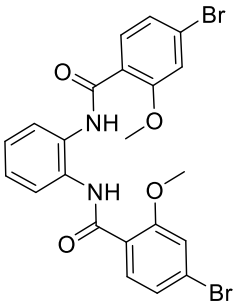

Eluent for column chromatography: 0.5% MeOH in $CHCl_3$; **Physical appearance:** White powder; Yield = 71%; **^{1}H NMR (400 MHz, $CDCl_3$)**: δ 9.67 (s, 2H), 8.16 (d, *J* = 8.4 Hz, 2H), 7.73 – 7.66 (m, 2H), 7.31 – 7.24 (m, 4H), 7.14 (d, *J* = 1.6 Hz, 2H), 3.88 (s, 6H); **^{13}C NMR (101 MHz, $CDCl_3$)**: δ 163.43, 158.02, 134.00, 131.33, 127.66, 126.60, 126.20, 124.91, 120.35, 115.24, 56.44; **IR ($\tilde{\nu}$ cm^{-1})**: 3344.33, 3303.48, 1662.15, 1585.99, 1533.41, 1509.69, 1465.97, 1394.14, 1235.95, 1179.69, 1016.26**,** 896.43, 845.74, 759.46; **HRMS (ESI)**: m/z $[M+H]^+$ Calc. for $C_{22}H_{18}Br_2N_2O_4$:532.9712 ; Found: 532.9717.

***N*,*N*'-(1,2-phenylene)bis(3-methoxy-2-naphthamide) (5c)**

Eluent for column chromatography: 30% EtOAc in petroleum ether; **Physical appearance:** Light yellow powder; Yield = 42**%**; **^{1}H NMR (400 MHz, $CDCl_3$)**: δ 9.99 (s, 2H), 8.88 (s, 2H), 7.92 (d, *J* = 8.1 Hz, 2H), 7.88 (dt, *J* = 7.2, 3.6 Hz, 2H), 7.74 (d, *J* = 8.2 Hz, 2H), 7.57 – 7.51 (m, 2H), 7.45 – 7.38 (m, 2H), 7.35 – 7.29 (m, 2H), 7.21 (s, 2H), 3.89 (s, 6H); **^{13}C NMR (101 MHz, $CDCl_3$)**: δ 164.06, 154.76, 136.06, 134.54, 131.26, 129.33, 128.73, 128.35, 126.39, 126.30, 125.79, 124.89, 122.25, 106.74, 55.99; **IR ($\tilde{\nu}$ cm^{-1})**: 3330.83, 3294.31, 3046.51, 2935.21, 1660.78, 1625.94, 1592.86, 1530.95, 1482.12, 1455.18, 1453.55, 1170.52, 1072.64, 1006.18, 827.14, 746.23, 703.76, 654.22; **HRMS (ESI)**: m/z $[M+H]^+$ Calc. for $C_{30}H_{24}N_2O_4$: 477.1814, Found: 477.1808.

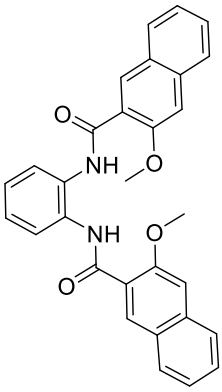

***N,N'*-(1,2-phenylene)bis(2-methoxy-4-(trifluoromethyl)benzamide) (5a)**

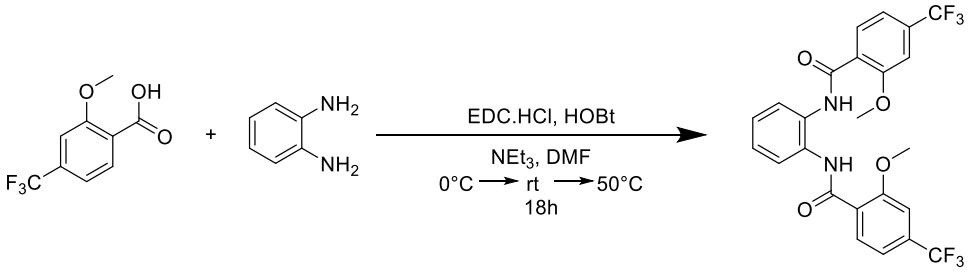

Procedure: To a solution of the substituted 2-methoxybenzoic acid (300 mg, 1.36 mmol, 3.5 eq) in DMF (9.5 mL) was added *o*-phenylenediamine (42 mg, 0.39 mmol,1 eq.) followed by Et_3N (215 µL,1.6 mmol,4 eq.), cooled to 0°C in an ice bath and stirred for 5 min. Then HOBt (189 mg, 1.4 mmol, 3.6 eq.) was added and the mixture stirred at 0 °C for 15 min. Finally, EDC·HCl (340 mg, 1.7 mmol, 4.5 eq.) was added and the mixture further stirred at 0°C for another 15 min. The mixture was then allowed to reach 50 °C stirred at this elevated temperature for next 18 h. It was then diluted with EtOAc and washed with water. The aqueous layer was further extracted with EtOAc (3 times), the organic layers combined, washed with brine, dried over anhydrous Na_2SO_4, and the solvent removed in vacuo. The residue was purified by silica gel column chromatography using 1% MeOH in chloroform as eluent to obtain the product as a white powder. Yield = 215 mg, 42%; **^{1}H NMR (400 MHz, $CDCl_3$)**: δ 9.78 (s, 2H), 8.41 (d, *J* = 7.9 Hz, 2H), 7.73 – 7.65 (m, 2H), 7.38 (d, *J* = 7.5 Hz, 2H), 7.36 – 7.28 (m, 2H), 7.21 (s, 2H), 3.96 (s, 6H); **^{13}C NMR (101 MHz, $CDCl_3$)**: δ 163.03, 157.74, 135.14 (q, *J* = 32.7 Hz), 133.50, 131.27, 126.85, 126.35, 124.43, 123.48 (q, *J* = 272.9 Hz), 118.19 (d, *J* = 3.7 Hz), 108.72 (q, *J* = 3.6 Hz), 56.43; **^{19}F NMR (377 MHz, $CDCl_3$)**: δ - 63.07; **IR ($\tilde{\nu}$ cm^{-1})**: 3346.49, 1673, 1598.01, 1538.36, 1458.71, 1413.51, 1328.34, 1232.93, 1171.04, 1124.56, 1020.86, 747.53; **HRMS (ESI)**: m/z $[M+H]^+$ Calc. for $C_{24}H_{18}F_6N_2O_4$: 513.1249, Found: 513.1253.

Synthesis of bissalicylamides through demethylation

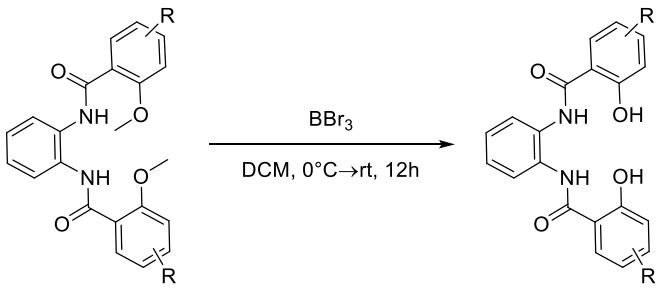

General Procedure D: To a 0°C cooled solution of substituted *o*-methylated bissalicylamides (1 eq) in DCM (8 mL) was added BBr_3 (1 M in DCM, 5.8 eq) drop wise. After the addition of BBr_3 the mixture was allowed to stir at room temperature (rt) for 12 h. The progress of the reaction was monitored using TLC. Once the reaction was done, DCM in the reaction mixture was evaporated using rota evaporator and kept the crude reaction mixture in an ice bath, followed by addition of methanol to quenched the excess BBr_3. Formation of precipitation will be observed upon addition of methanol, this methanol was evaporated in the rota evaporator and distilled water was added in the crude reaction mixture. The precipitation was collected using a vacuum filter and was dried inside desiccator for 18 h.

***N*,*N*'-(1,2-phenylene)bis(4-bromo-2-methoxybenzamide) (2b)**

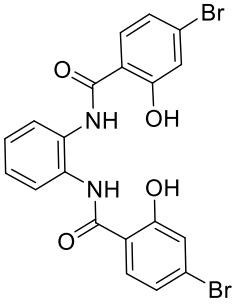

Physical appearance: White powder; yield = 78%; **^{1}H NMR (400 MHz, DMSO-*d*$_6$)**: δ 12.05 (s, 2H), 10.36 (s, 2H), 7.93 (d, *J* = 8.3 Hz, 2H), 7.80 (dd, *J* = 5.7, 3.6 Hz, 2H), 7.28 (dd, *J* = 6.0, 3.6 Hz, 2H), 7.21 – 7.15 (m, 4H); **^{13}C NMR (101 MHz, DMSO-*d*$_6$)**: δ 165.29, 158.70, 131.71, 130.96, 126.58, 125.93, 125.40, 122.55, 119.84, 116.89; **IR(ṽ cm^{-1})**: 3344.33 ,3303.48, 1662.15, 1585.99, 1533.41, 1509.69, 1465.97, 1394.14, 1235.95, 1179.69, 1016.26**,** 896.43, 845.74, 759.46**; HRMS (ESI)**: m/z $[M+H]^+$ Calc. for: $C_{20}H_{14}Br_2N_2O_4$: 504.9399, Found: 504.9393.

***N,N'*-(1,2-phenylene)bis(2-hydroxy-4-(trifluoromethyl)benzamide) (2a)**

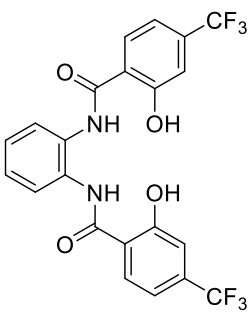

Physical appearance: white powder; yield = 99% ; **^{1}H NMR (400 MHz, DMSO-*d*$_6$)**: δ 12.04 (s, 2H), 10.47 (s, 2H), 8.18 (d, *J* = 8.1 Hz, 2H), 7.82 (dd, *J* = 5.7, 3.6 Hz, 2H), 7.31 (dd, *J* = 9.2, 6.0 Hz, 6H); **^{13}C NMR (101 MHz, DMSO-*d*$_6$)**: δ 164.59, 157.70, 133.06 (q, *J* = 31.6 Hz), 131.42, 130.89 , 125.99 , 125.40 , 123.53 (q, *J* = 272.8 Hz), 121.56 , 115.62 (d, *J* = 3.4 Hz), 113.78 (d, *J* =

3.6 Hz); **^{19}F NMR (377 MHz, DMSO-*d*$_6$)**: δ - 62.36 ; **IR(ṽ cm^{-1})**: 3293.48, 1648.96, 1602.85, 1551.94, 1515.13, 1334.28, 1120.48, 752.04**; HRMS (ESI)**: m/z $[M+H]^+$ Calc. for $C_{22}H_{14}F_6N_2O_4$: 485.0936, Found: 485.0939.

***N,N'*-(1,2-phenylene)bis(3-hydroxy-2-naphthamide) (2c)**

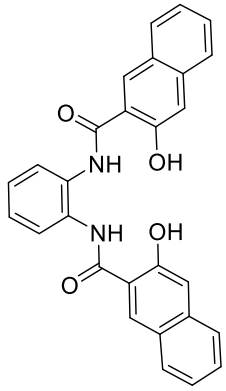

Physical appearance: white powder; yield = 44%; **^{1}H NMR (400 MHz, DMSO-*d*$_6$)**: δ 10.69 (s, 2H), 8.66 (s, 2H), 8.00 – 7.79 (m, 4H), 7.73 (d, *J* = 8.3 Hz, 2H), 7.51 (t, *J* = 7.4 Hz, 2H), 7.38 – 7.25 (m, 6H) .**^{13}C NMR (101 MHz, DMSO- *d*$_6$)**: δ 165.79, 154.05, 136.19, 131.72, 131.33, 129.12, 128.58, 127.08, 126.01, 125.89, 125.51, 124.01, 120.30, 110.95. **IR (ṽ cm^{-1})**: 3050.28, 1623.08, 1597.99, 1523.39, 1449.61, 1358.21, 1210.24, 874.52, 770.98, 746.24, **HRMS (ESI)**: m/z $[M+H]^+$ Calc. for $C_{28}H_{20}N_2O_4$: 449.1501; Found: 449.1499.

Synthesis of Phenylboronic ester substituted bissalicylamides

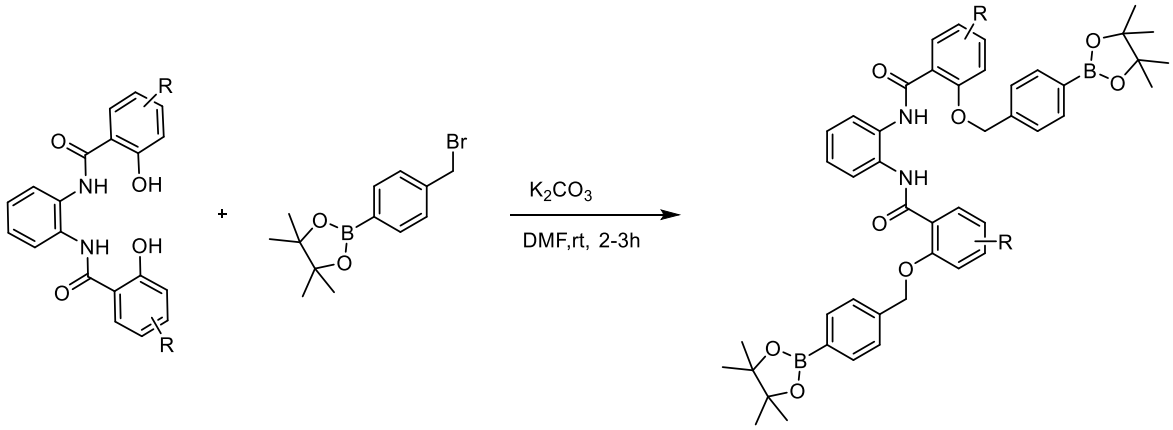

General procedure: To a stirred solution of substituted bissalicylamide in DMF, K_2CO_3 was added at room temperature (rt) and the reaction mixture stirred for 2 to 3 h. The crude reaction mixture was then poured into water and extracted using EtOAc (3 times). The organic layers were then combined, dried using anhydrous sodium sulphate and solvent removed *in vacuo*. The mixture was purified through preparative HPLC on a reverse phase column with water/ acetonitrile system as the mobile phase.

***N*,*N*'-(1,2-phenylene)bis(4-bromo-2-((4-(4,4,5,5-tetramethyl-1,3,2-dioxaborolan-2-yl)benzyl)oxy)benzamide) (1b)**

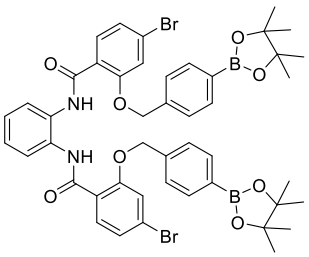

Eluent for preparative HPLC: 90% Acetonitrile in water**; Physical appearance:** White powder; **Yield =** 78%; **^{1}H NMR (400 MHz, $CDCl_3$)**: δ 9.72 (s, 2H), 7.97 (d, *J* = 8.4 Hz, 2H), 7.74 (d, *J* = 8.0 Hz, 4H), 7.48 (dd, *J* = 6.0, 3.6 Hz, 2H), 7.25 (s, 2H), 7.23 (s, 2H), 7.22 – 7.16 (m, 2H), 7.11 (dd, *J* = 8.4, 1.7 Hz, 2H), 6.99 (d, *J* = 1.6 Hz, 2H), 5.14 (s, 4H), 1.35 (s, 24H); **^{13}C NMR (101 MHz, $CDCl_3$)**: 163.51, 156.92, 137.98, 135.45, 133.81, 131.14, 127.26, 126.38, 126.14, 125.73, 125.06, 120.93, 116.62, 84.11, 71.41, 25.05; **IR (ṽ , cm^{-1})**: 3348.04, 2981.49, 1704.85, 1660.4, 1558.21, 1516.26, 1397.99, 1356.46, 1319.39, 1269.74, 1139.95. **MALDI**: m/z $[M+K]^+$ Calc. for: $C_{46}H_{48}B_2Br_2KN_2O_8$: 977.1, Found: 977.6.

***N*,*N*'-(1,2-phenylene)bis(2-((4-(4,4,5,5-tetramethyl-1,3,2-dioxaborolan-2-yl)benzyl)oxy)-4-(trifluoromethyl)benzamide) (1a)**

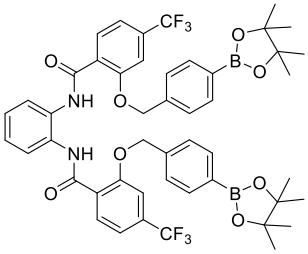

Eluent for preparative HPLC: 95% Acetonitrile in water; **Physical appearance:** White powder; **Yield =** 45%; **^{1}H NMR (400 MHz, DMSO-d_6)**: δ 11.75 (s, 1H), 10.43 (s, 1H), 8.01 (dd, *J* = 8.2, 1.4 Hz, 1H), 7.80 (dd, *J* = 5.9, 3.6 Hz, 1H), 7.43 (td, *J* = 8.1, 1.6 Hz, 1H), 7.32 – 7.25 (m, 1H), 7.05 – 6.90 (m, 2H); **^{13}C NMR (101 MHz, $CDCl_3$)**: δ 163.14, 156.52, 137.72, 135.46, 134.72 (q, *J* = 32.7 Hz), 133.26, 130.91, 129.58, 126.55 126.28, 125.70, 125.19, 123.39 (q, *J* = 273.9 Hz), 118.34 (d, *J* = 3.6 Hz), 110.09 (q, *J* = 3.0 Hz), 84.13, 71.46, 25.01; **IR (ṽ , cm^{-1})**: 3339.81, 2983.95, 1660.74, 1611.62, 1513.77, 1360.38, 1324.09, 1170.32, 1132.22, 1091.53, 1009.06; **MALDI**: m/z $[M+K]^+$ Calc. for: $C_{48}H_{48}B_2F_6KN_2O_8$: 955.3, Found: 955.8.

***N*,*N*'-(1,2-phenylene)bis(3-((4-(4,4,5,5-tetramethyl-1,3,2-dioxaborolan-2-yl)benzyl)oxy)-2-naphthamide) (1c)**

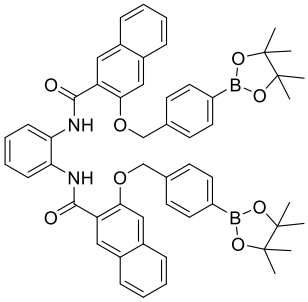

Eluent for preparative HPLC: 95% Acetonitrile in water; **Physical appearance:** White powder; **Yield =** 75%; **^{1}H NMR (400 MHz, $CDCl_3$)**: δ 10.00 (s, 2H), 8.67 (s, 2H), 7.77 (d, *J* = 8.1 Hz, 2H), 7.67 (d, *J* = 8.0 Hz, 4H), 7.64 – 7.56 (m, 4H), 7.51 – 7.43 (m, 2H), 7.39 – 7.32 (m, 2H), 7.26 – 7.20 (m, 6H), 7.10 (s, 2H), 5.21 (s, 4H), 1.34 (s, 24H); **^{13}C NMR (101 MHz,**

$CDCl_3$): δ 164.31, 153.67, 138.78, 135.85, 135.32, 134.23, 131.33, 129.28, 128.50, 128.44, 126.45, 126.26, 126.12, 125.66, 124.82, 122.96, 108.48, 84.01, 71.08, 25.03; **IR ($\tilde{\nu}$, cm^{-1})**: 3340,2981.54, 1658.89, 1511.59, 1450.15, 1397.86, 1354.69, 1264.04, 1208.28, 1140.53, 1080.2; **MALDI**: m/z $[M+K]^+$ Calc. for: $C_{54}H_{54}B_2KN_2O_8$: 919.3; Found: 919.8.

3.4 Activation Experiments

i. TLC experiment

For this experiment, 1 mM stock solutions of the protransporters were prepared in 1:1 solution of acetonitrile and methanol. In this stock solution, 9.8 M (30% hydrogen peroxide) H_2O_2 was added in such a way that the final concentration of H_2O_2 amount to 10 equivalent of the compound. Then it was kept in the dark environment without any disturbance at room temperature for 48 h before spotting on the TLC.

To confirm the regeneration of the ion transporter the reference for transporter (**2b** and **2c**) and inactive protransporter (**1b** and **1c**) was spotted on **1**and **2** respectively and the activated protransporter solution was spotted on **3** (see **Figure 4**) and ran the TLC in 25% ethyl acetate in hexane. And the regeneration of transporter was observed under UV light of 254 nm wavelength.

ii. MALDI

A 2.5 mM protransporter stock solution was prepared in HPLC grade DMSO and 9.8 M (30% hydrogen peroxide) was added in such a way that the equivalents of the protransporter and hydrogen peroxide is in 1:2 ratio. This mixture was kept in dark environment for 30 h without any disturbance at room temperature. Finally, this solution was poured into a 15 mL falcon tube and a mini work up was performed by adding distilled water and excess ethyl acetate. This ethyl acetate layer was used for the mass analysis in MALDI.

iii. HRMS

The same activated solution from the TLC experiment above was used for the mass analysis and the regeneration the transporter was observed.

3.5 Chloride ion transport study

i. Preparation of EYPC-LUVs⊃lucigenin

In a clean dry 10 mL round bottom flask, 1 mL of egg yolk phosphatidylcholine (EYPC, 25 mg/mL in chloroform) was taken and a thin film was made by evaporating the chloroform with nitrogen gas. The round bottom flask was covered with aluminium foil and kept in high vacuum for 4 h to remove the trace amount of chloroform. The dried film was hydrated with a solution of sodium nitrate (200 mM, Lucigenin = 1 mM) solution. The following mixture was then subjected to vortex 6 times periodically in an interval of 10 min. This hydrated mixture was put in a freeze-thaw cycle (liquid nitrogen, 55 ºC) of 11 cycles. The resulting suspension was extruded 35 times using 200 nm pore size polycarbonate membrane. Finally, the extravesicular lucigenin dye was removed through size exclusion column using stationary phase Sephadex G-50 and mobile phase 200 mM sodium nitrate. The resultant vesicles were diluted to 6 mL to get the EYPC-LUVs⊃lucigenin. Final condition: ≈ 5 mM EYPC; Inside: 1 mM lucigenin, 200 mM $NaNO_3$; Outside: 200 mM $NaNO_3$.

ii. Stock preparation

All the stock preparation was done using HPLC grade Acetone and the mili-Q water.

iii. Activation for lucigenin assay

The activation was done by adding H_2O_2 10 times the concentration of compound in the stock solution and was kept at 25 ºC in a dark environment without any disturbance for the required duration of time.

iv. Procedure for lucigenin assay

In a clean cuvette 1975 µL of 200 mM $NaNO_3$ and 25 µL of the EYPC-LUVs⊃lucigenin vesicle (prepared above) was added and kept under stirring of 900 rpm inside a fluorescence instrument at t = 0. The time dependent fluorescence emission intensity of lucigenin was recorded at λ_{em} = 535 nm (λ_{ex} = 455 nm). To create a gradient of Cl^- ion concentration between the intra and extra vesicular environment 33.33 µL of 2 M NaCl was added at t = 20 s. Since the gradient is created the desired compound with the required amount is added at t = 100 s. and finally the vesicle is lysed by adding 25 µL 10% triton X-100 was added at t = 300 s, which will destroy the vesicle resulting the fluorescence to quenched.as the lucigenin is exposed to the higher concentration of chloride in the extravesicular environment.

The fluorescence intensity data acquired from the lucigenin assay is normalised using the equation S1

$$I_F = [(I_t - I_0)/(I_\infty - I_0)] \times (-100) \qquad \text{(Equation S1)}$$

Where I_0 is the initial intensity (just before transporter addition), I_t is the intensity at time t, and I_∞ the final intensity after the addition of Triton X-100.

3.6 Biological studies

i. Cell culture condition

For the biological experiments the MCF-7 breast cancer cell line was used. The cell culture was done in high glucose Dulbecco's modified Eagle media (DMEM) containing 2 mM L-glutamine. The media was supplemented with 10% (v/v) heat-inactivated fetal bovine serum (FBS), 100 units/mL penicillin, and 100 µg/mL streptomycin. The cultures were incubated 37 ºC in a humidified incubator (Eppendorf) supplied with 5% CO_2.

ii. MTT assay

The purpose of this assay is to check the cytotoxicity of our transporters and protransporters, which will let us know if our compounds have a potential to be a cancer drug or not. The detail concept of MTT assay is given in the biological studies part of results and discussion. As for the protocol, we take a tissue culture treated 96 well plate, added PBS buffer in all the outermost wells of the plates (see **Figure: 3**) to reduce the evaporation rate in other wells. And seeded the remaining well with density of 8×10^3 cell/well/100 µL in complete DMEM media and allow it to recover at 37 ºC in a humidified 5% CO_2 incubator for 24 h. After incubation, on the following day control, protransporter and transporter were added in the preferred wells and the similar incubation condition as before was continued for another 24 h. Post second incubation the media was removed and 100 µL (0.5 mg/mL) in MTT solution in DMEM was added and incubated for 4 h. Finally all the media are removed, DMSO was added in each well to dissolve the formazan crystals and absorbance was measured at 570 nm. The absorbance data was converted in percentage form and compared with the Untreated well (The untreated wells having only DMSO for control experiment was set as 100% and scaled the remaining wells accordingly).

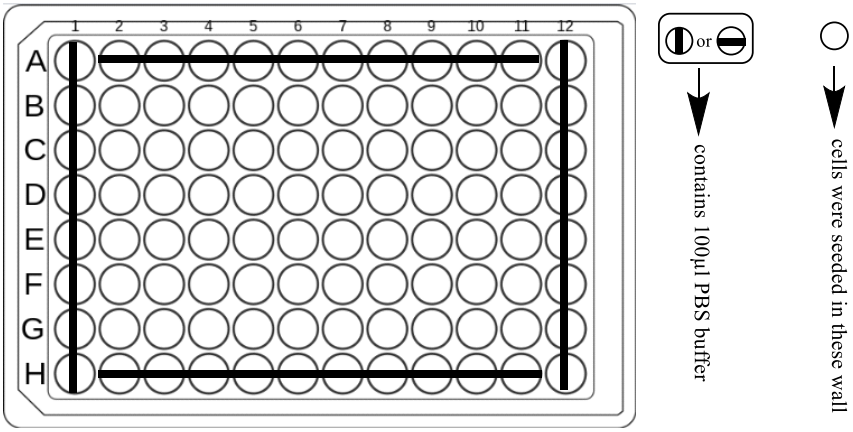

Figure 3: Layout of the 96 well plate for MTT assay

4. Results and Discussion

Synthesis of Phenyl boroester linked substituted Bis-salicylamide. We have synthesized and characterized three derivatives of the required protransporter and the transporter. The protransporters were found to be sensitive in silica, as a result the purification of the protransporter (see last step of **Scheme 2**) was performed in reverse phase C-18 column (stationary phase) and eluted using a solvent mixture of acetonitrile and water (mobile phase) in combiFlash. All the transporters were found to be very stable even at room temperature. But when it comes to protransporter **1a** was found to start degrading in two weeks even at 0 ºC.

Evaluation of response from the protransporter in the presence of hydrogen peroxide by using TLC, MALDI and HRMS techniques. One of the main goals in this project is to show that the protransporter can indeed get activated in the presence of H_2O_2 and converts to transporter. And this was confirmed through TLC, MALDI and HRMS (stock preparation of all these techniques are given in material and methods section). In **Figure 4**, three different spot **1**, **2** and **3** are observed with transporter, protransporter and protransporter after activation with the H_2O_2 on the TLC and we can clearly see the regeneration of the transporter in **3** which confirms the regeneration of the transporter.

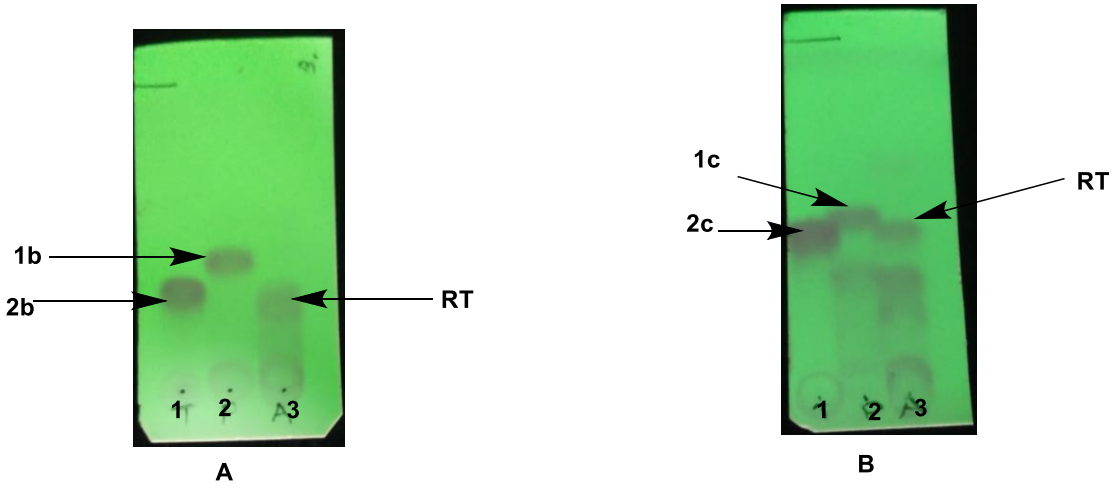

Here,

1 =Transporter, **2 =** Protransporter, **3 =** Activated protransporter with H_2O_2,
A = TLC of Br^- derivative, **B** = TLC of Nap derivative, **RT** = Regenerated transporter spot

Figure 4: Confirmation for the regeneration of transporter from the protrasnporter.

The TLC experiment was further supported in MALDI spectra in **Figure 5**. In the MALDI spectra we can see all the mass peak of the single phenyl boroester linked transporter as well, indicating that it requires two steps of activation to generate the transporter.

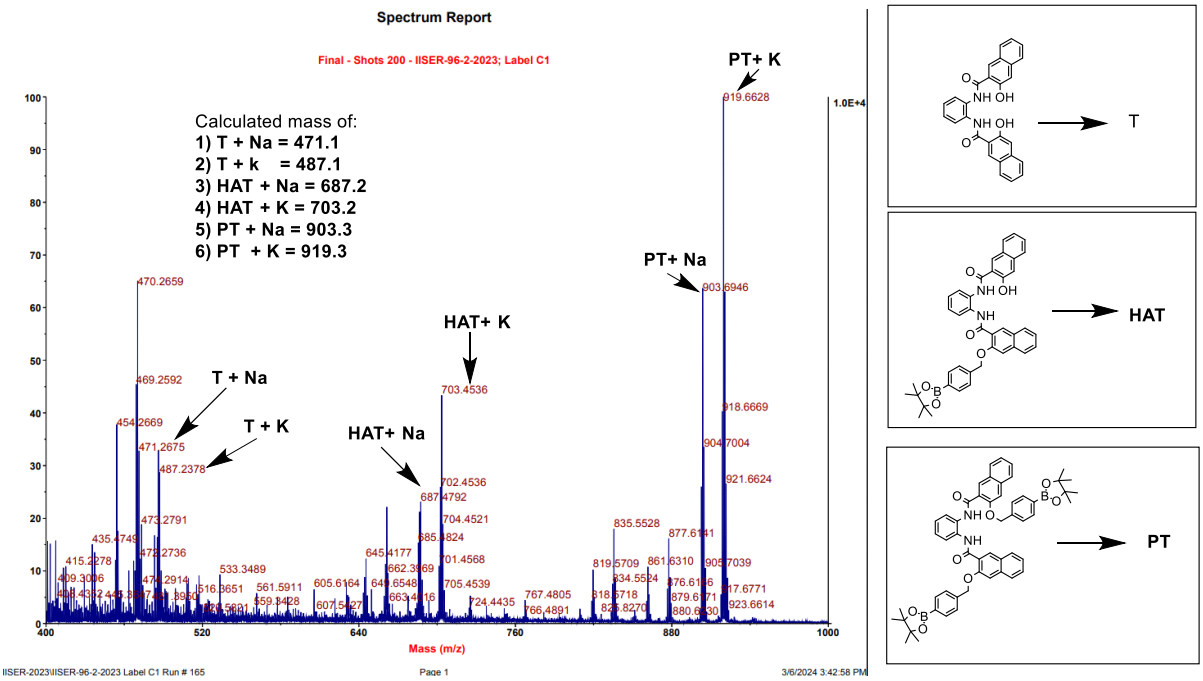

Figure 5: MALDI spectra for the activation of **1c** with H_2O_2.

Finally, we found the regeneration of transporter after activation in high resolution mass spectrometry (HRMS) as well.

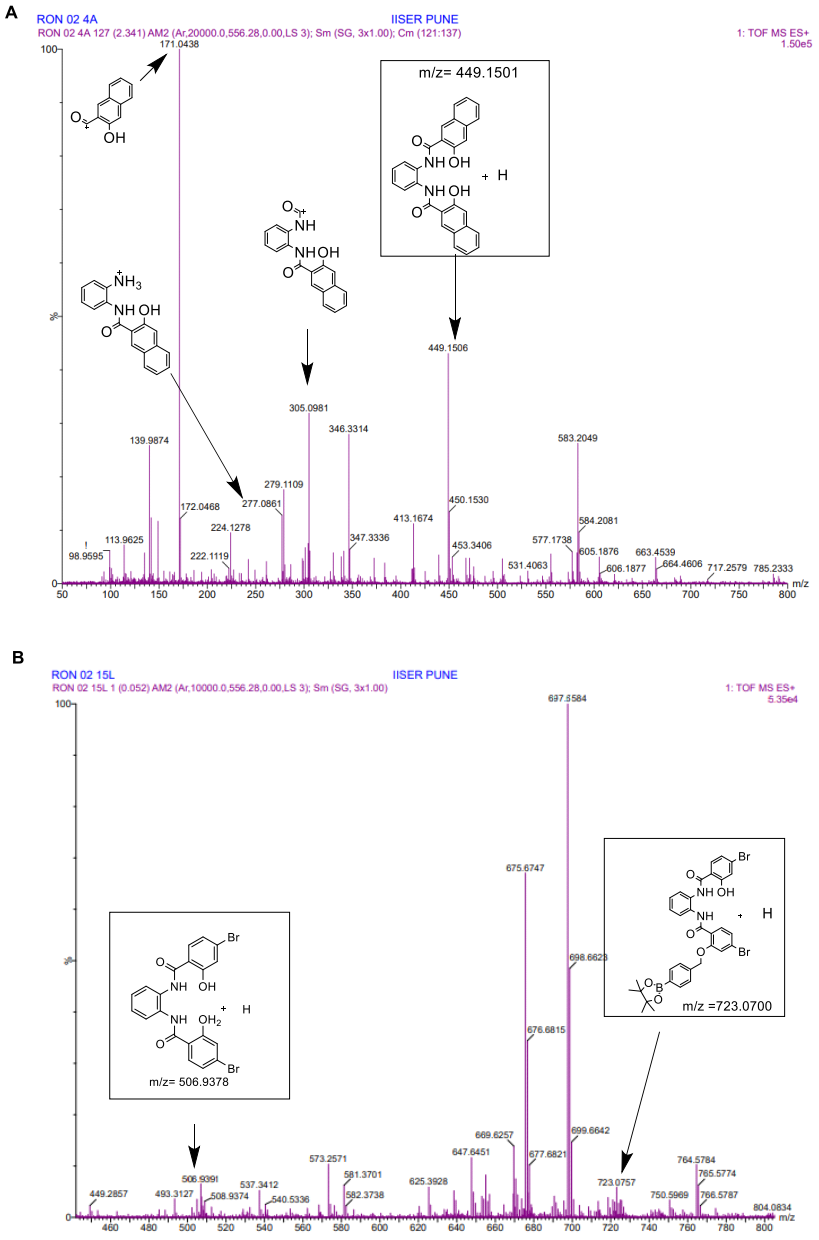

Figure 6: Confirmation of regeneration of the **2c** from **1c** through HRMS (**A**). Confirmation of regeneration of the **2b** from **1b** through HRMS (**B**).

Chloride ion transport estimation using lucigenin assay. The ultimate objective of the protransporters is to be inactive and upon activation it should be able transport the ions.

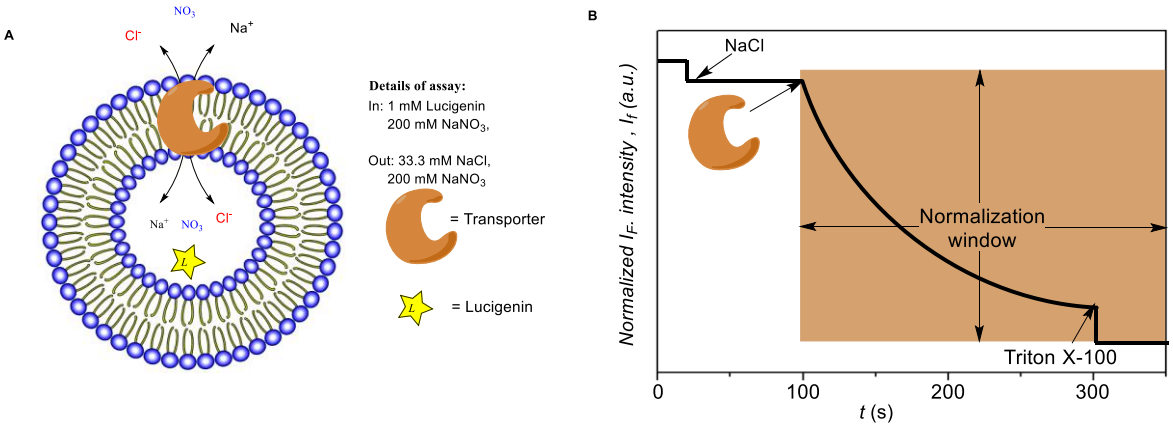

Figure 7: Schematic of fluorescence-based assay of ion transporter activity using EYPC-LUVs⊃lucigenin (**A**), and representative diagram of ion transport kinetics depicting the normalization window (**B**).

As the main focus of our compound is in the development of cancer drug, chloride ion is expected to transport by the generated transporter. As higher concentration of chloride ion in the cancer cell is already reported to trigger apoptotic cell death[9]. Thus the regain of chloride ion transport upon activation with H_2O_2 from the inactive form of protransporter was evaluated using lucigenin assay.

Lucigenin is a chloride sensitive dye. The fluorescence emission of the lucigenin dye gets quenched when it gets exposed to the chloride ions by charge transfer process.[10] The idea of this assay is to prepare a vesicle that entraps lucigenin dye (and 200 mM sodium nitrate). Dilute mixture of the following vesicle in 200 mM sodium sulphate solution will undergo time based fluorescence emission intensity measurement (see procedure for lucigenin assay in methods section). During the measurement a pulse of NaCl will be given at t = 20 s, which will create a Chloride ion gradient between the intra and extra vesicular environment. Now the compound of interest will be added at t = 100 s. If the compound is able to transport chloride ion from the extra to intra vesicular environment, lucigenin will get exposed to the chloride entering the vesicle as a result the fluorescence will get quenched. This is how we confirm the ability of a compound to transport chloride ion through the bilayer membrane in the model system of EYPC-LUVs⊃lucigenin. If the compound is found to transport chloride ion in this model system then we will take the compound the real cellular environment.

We have tried the lucigenin assay using active transporter (**1b** and **1c**) and found the transport activity. In both the graph in **A** and **B** of **Figure 8** the black line plot represents the activity of the transporter.

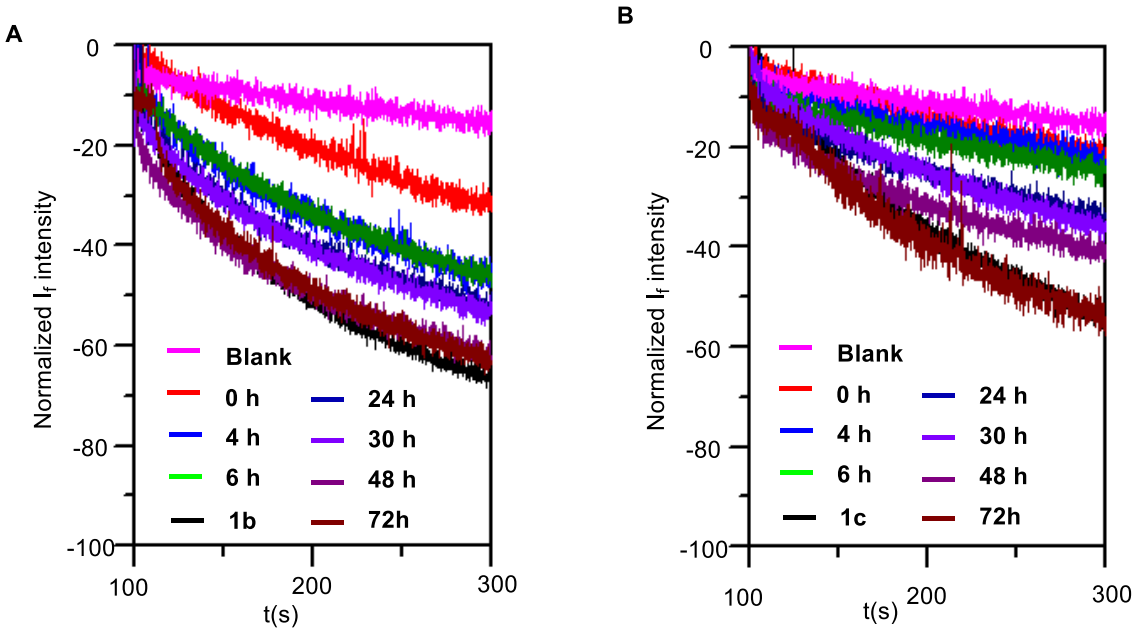

Figure 8: The no. of hours given in the legends of both the graph indicates the time after the addition of 10X equivalents of H_2O_2 in the stock solution. Regeneration of the chloride ion transport in the **1b** at 5.5 µM concentration (**A**). Regeneration of the chloride ion transport in the **1c** at 5.5 µM concentration (**B**).

Furthermore, in **Figure 8** the plot of the protransporter after activating with H_2O_2 is observed and found the transport ability to increasing over time, indicating that the chloride transport activity can be regain upon activation.

Evaluation of cytotoxicity for the transporter and protransporters in MCF-7 breast cancer cells. For the evaluation of cytotoxicity we performed the MTT assay (Protocol is given in the general methods section). MTT chemically 3-(4,5-dimethylthiazol-2yl)-2,5-diphenyltetrazolium bromide is used as an indicator of cell viability for this assay. In the MTT assay we measure the cell viability in term of the reductive activity of enzymatic conversion of tetrazolium compounds to water insoluble formazan crystals by dehydrogeneses found in the mitochondria of the living cell.[11] MTT is water soluble yellow coloured compound while on the other hand formazan is purple in colour and water insoluble. During the MTT treatment to the cells, if the cells are alive then the mitochondrial dehydrogeneses will convert the MTT to purpled coloured water insoluble formazan crystal (soluble in DMSO). Upon removal of the media followed by adding of DMSO (see protocol in general method section) formazan will get dissolved and a bright purple coloured solution is formed. However, if the cells are dead all the MTT will remain as it is, dissolved in the media. So, during the media removal process MTT goes with it and adding DMSO will just result to the colourless DMSO solution. Formazan has an absorbance at 570 nm[12]

and the cell viability is measured by comparing the absorbance of the compound treated well and untreated wells of the 98-well plate.

Proceeding ahead with the idea of the protransporter being inactive in model system (vesicles) and upon activating with H_2O_2 it was able to recover its transport activity, we tried our transporter and protransporter in the cellular environment and checked the cytotoxicity using MTT assay. For the MTT assay we used the breast cancer cell line MCF-7. And upon treatment of **2b** for 24h was found to be active while **1b** and **1c** were found to be non-toxic to the cell at the conc. that we tried in **Figure 9**. During the time of this writing the optimization for the activation of protrasnporter is still underway.

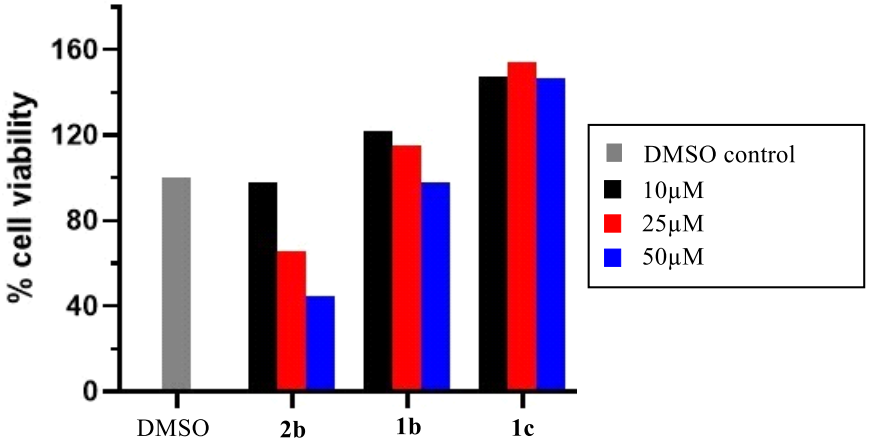

Figure 9: Cytotoxicity evaluation of **2b**, **1b and 1c** in different concentration through MTT assay.

5. NMR

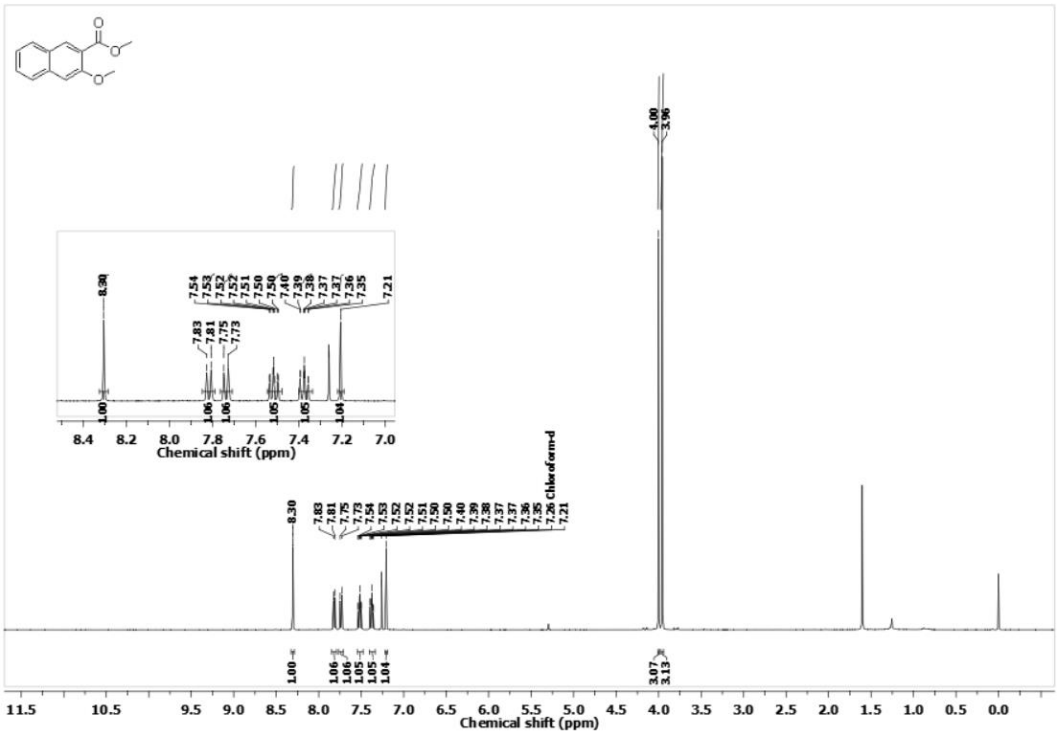

Figure 10: 400 MHz ^{1}H NMR spectrum of **7c** in $CDCl_3$. Solvent residual peak at 7.26 ppm.

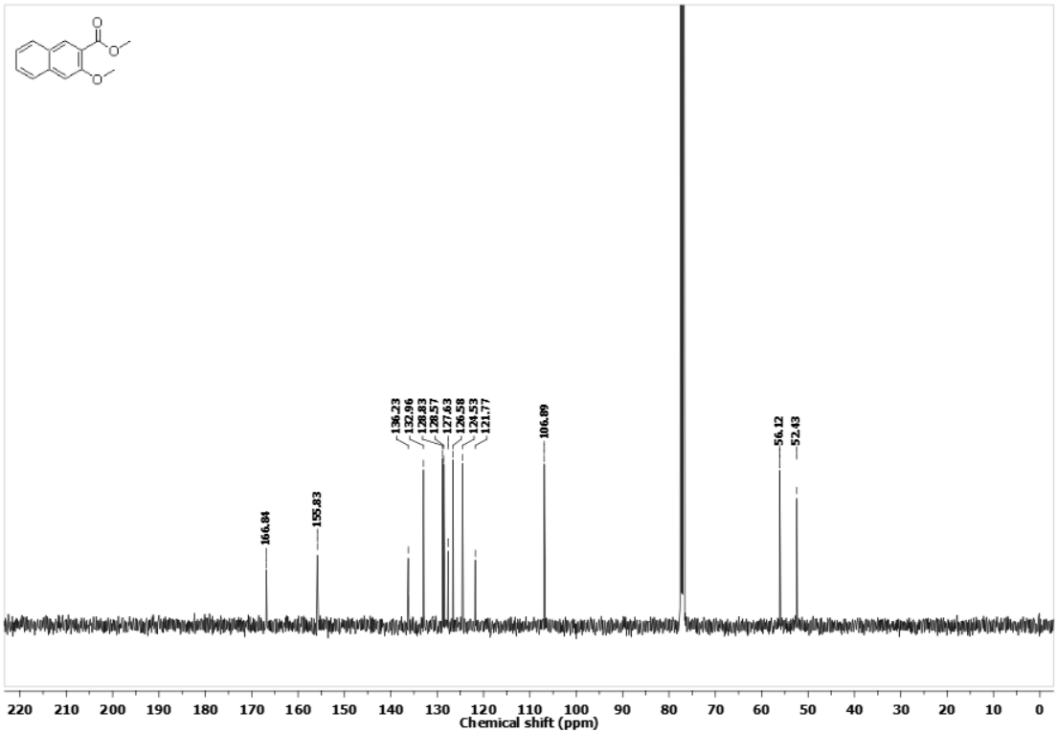

Figure 11: 101 MHz ^{13}C NMR spectrum of **7c** in $CDCl_3$. Solvent residual peak at 77.16 ppm.

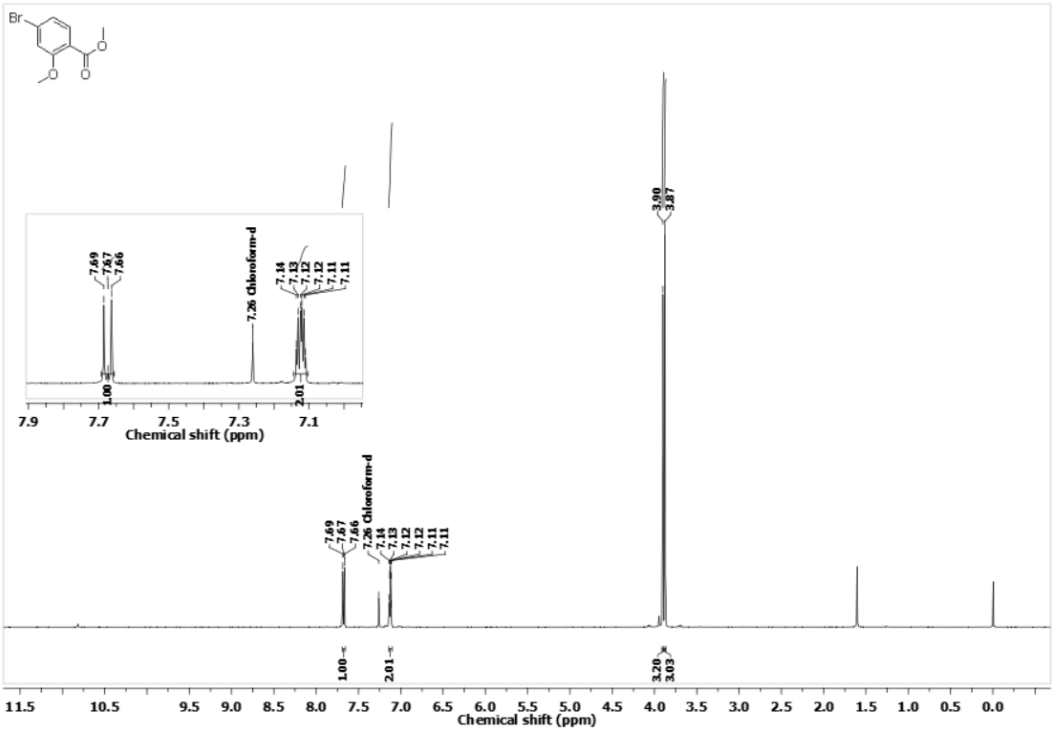

Figure 12: 400 MHz ^{1}H NMR spectrum of **7b** in $CDCl_3$. Solvent residual peak at 7.26 ppm.

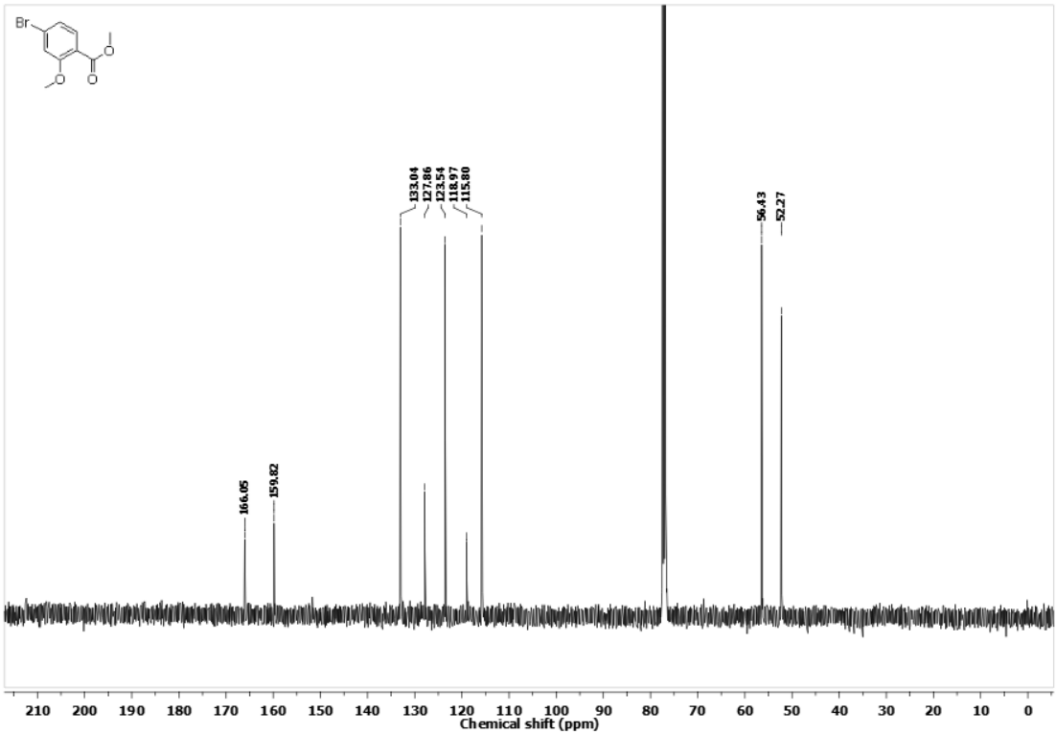

Figure 13: 101 MHz ^{13}C NMR spectrum of **7b** in $CDCl_3$. Solvent residual peak at 77.16 ppm.

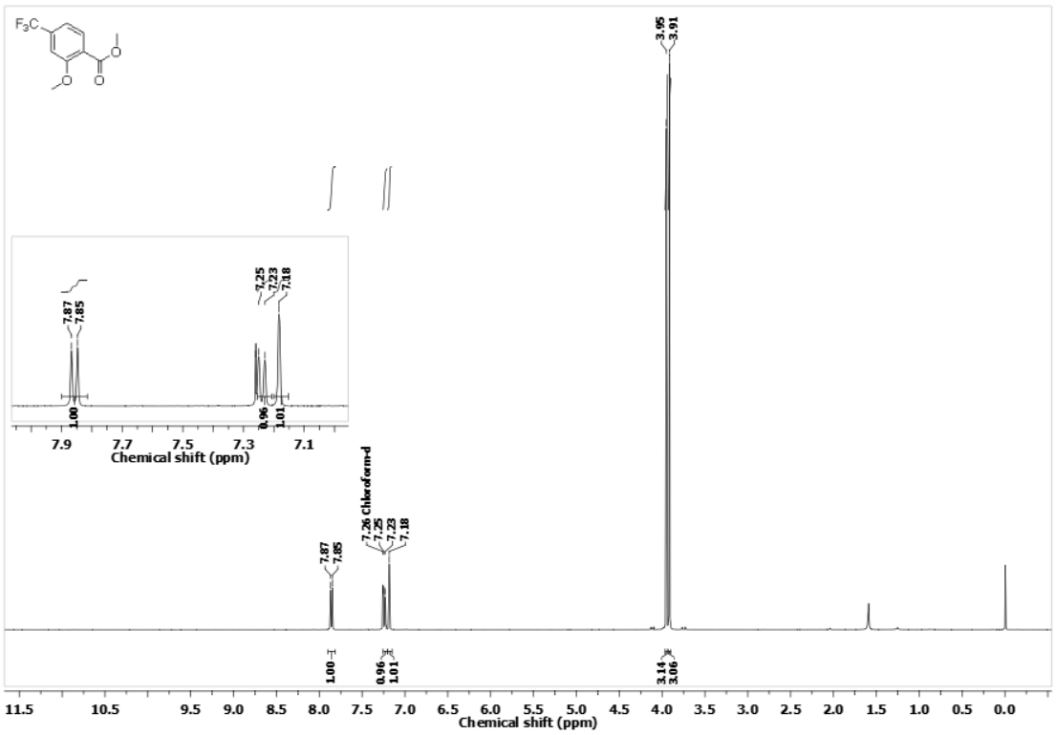

Figure 14: 400 MHz ^{1}H NMR spectrum of **7a** in $CDCl_3$. Solvent residual peak at 7.26 ppm.

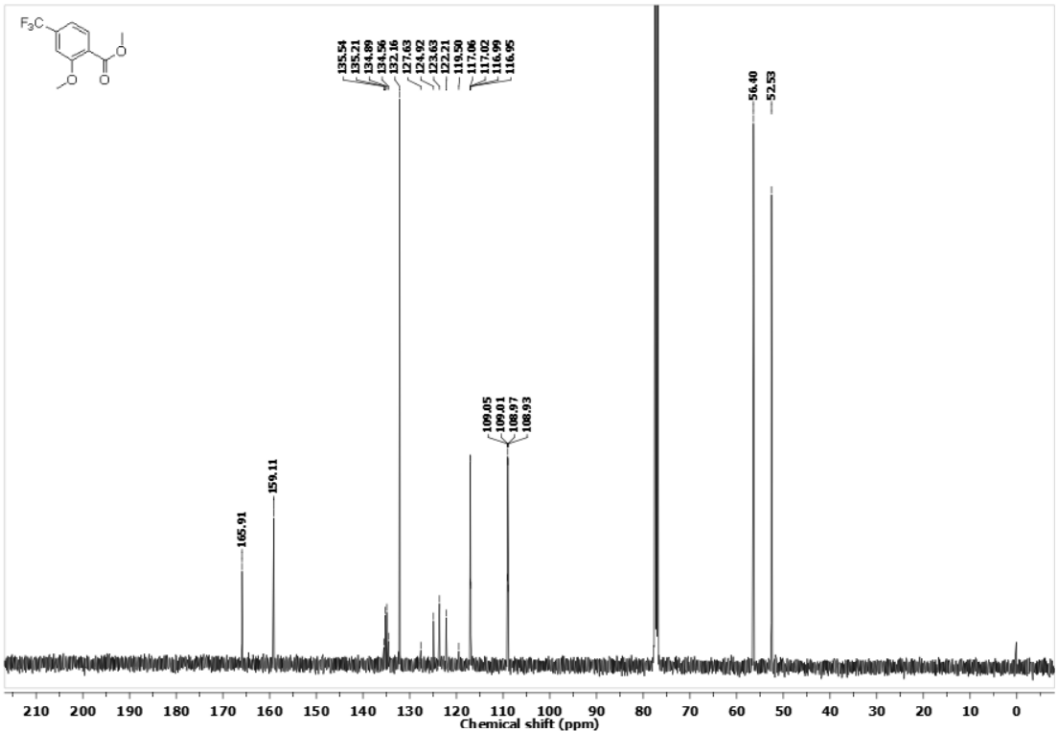

Figure 15: 101 MHz ^{13}C NMR spectrum of **7a** in $CDCl_3$. Solvent residual peak at 77.16 ppm.

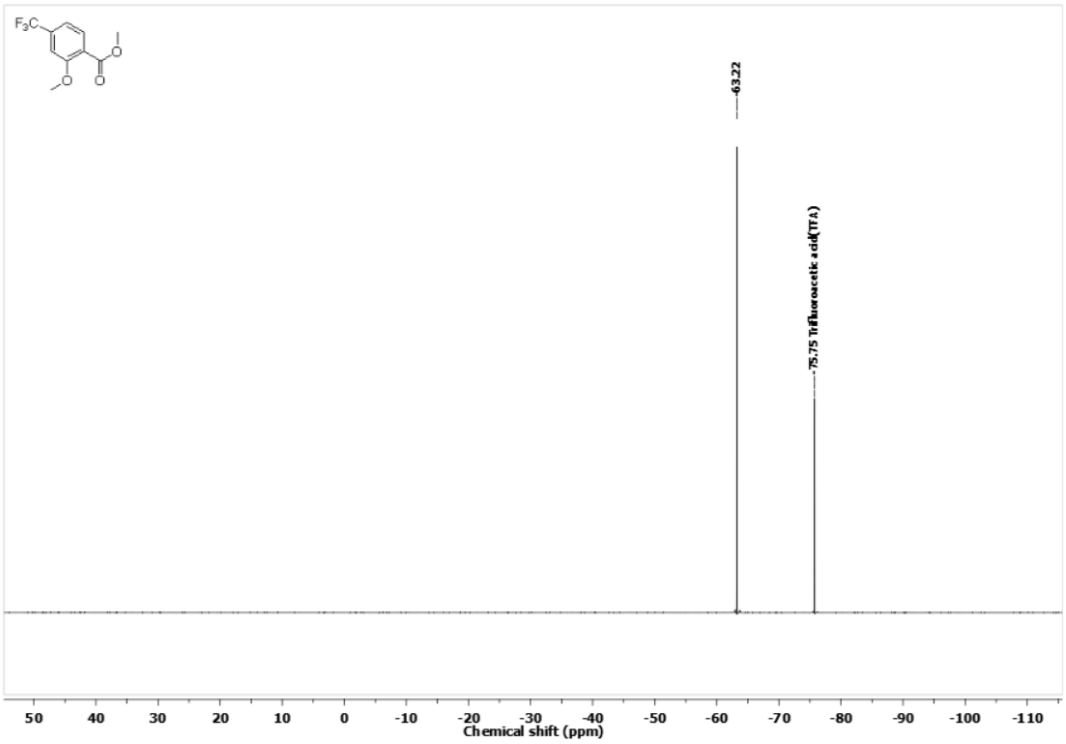

Figure 16: 377 MHz ^{19}F NMR spectrum of **7a** in $CDCl_3$. Internal reference peak at -75.75 ppm.

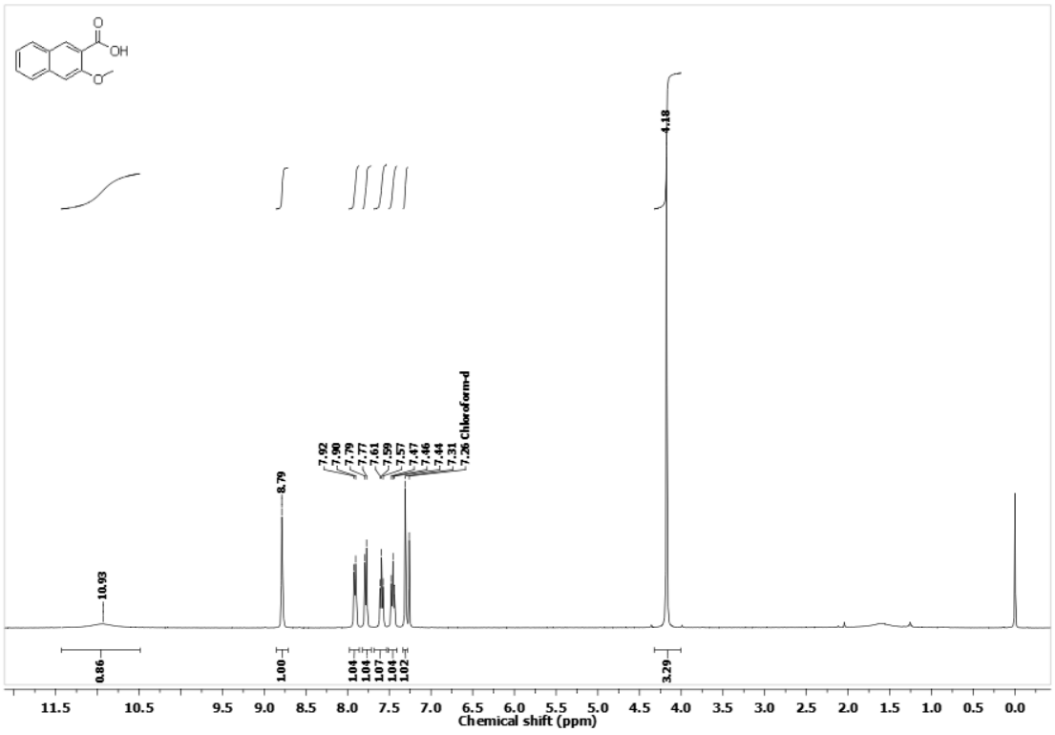

Figure 17: 400 MHz ^{1}H NMR spectrum of **6c** in $CDCl_3$. Solvent residual peak at 7.26 ppm.

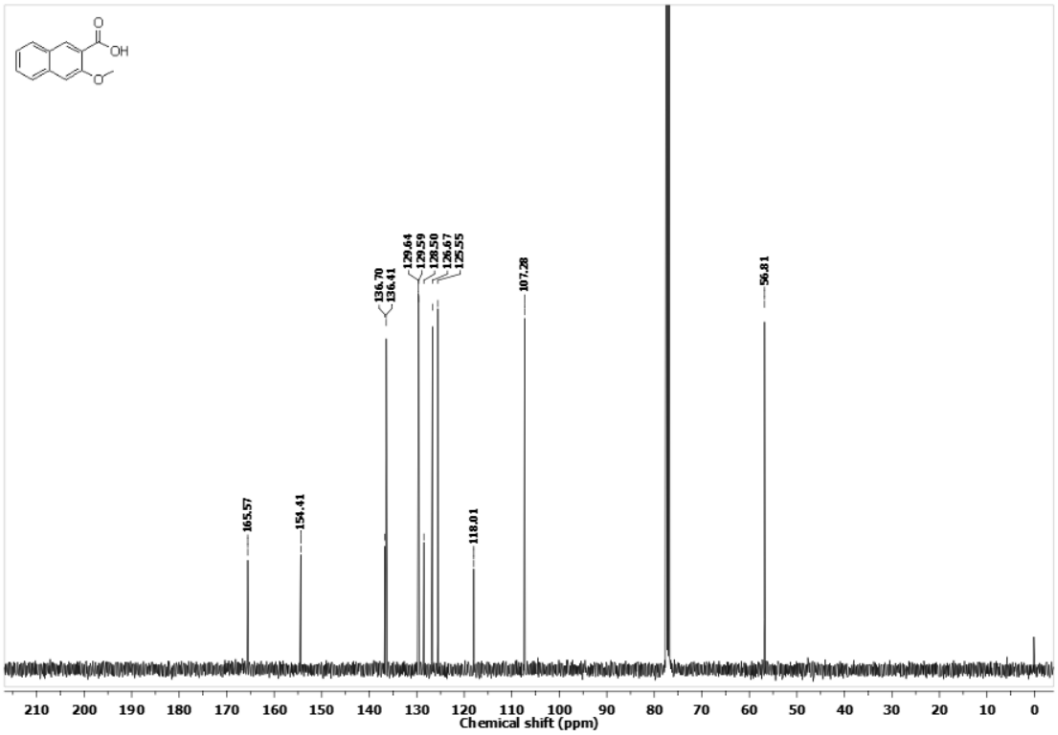

Figure 18: 101 MHz ^{13}C NMR spectrum of **6c** in $CDCl_3$. Solvent residual peak at 77.16 ppm.

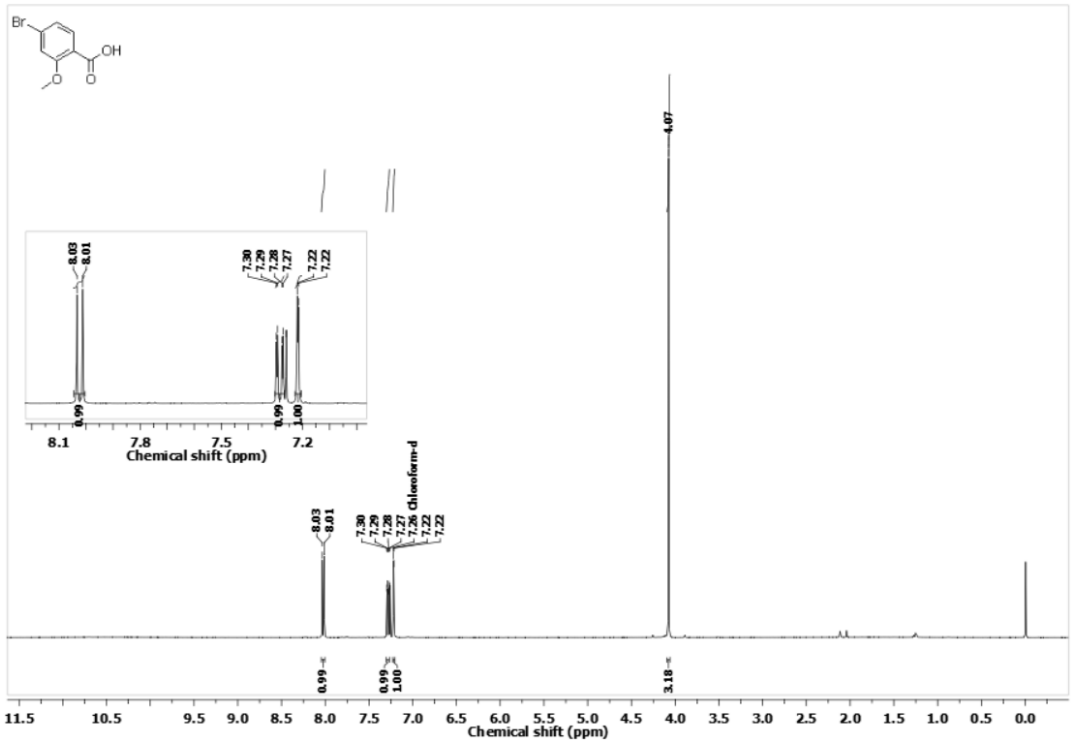

Figure 19: 400 MHz ^{1}H NMR spectrum of **6b** in $CDCl_3$. Solvent residual peak at 7.26 ppm.

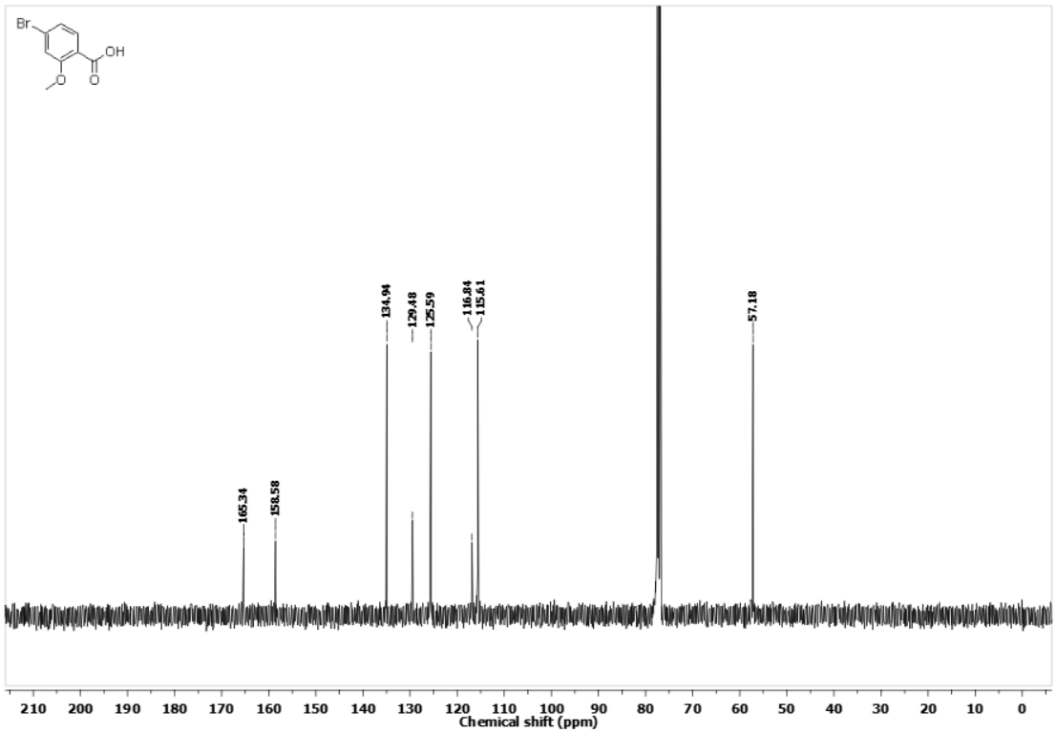

Figure 20: 101 MHz ^{13}C NMR spectrum of **6b** in $CDCl_3$. Solvent residual peak at 77.16 ppm.

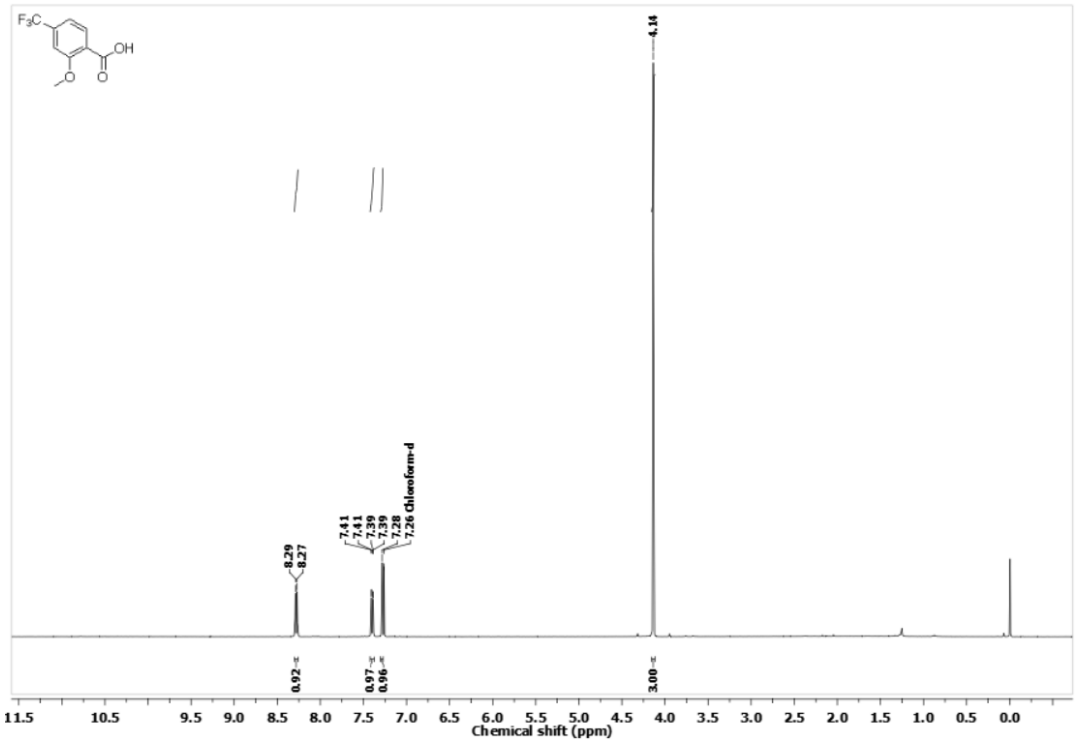

Figure 21: 400 MHz ^{1}H NMR spectrum of **6a** in $CDCl_3$. Solvent residual peak at 7.26 ppm.

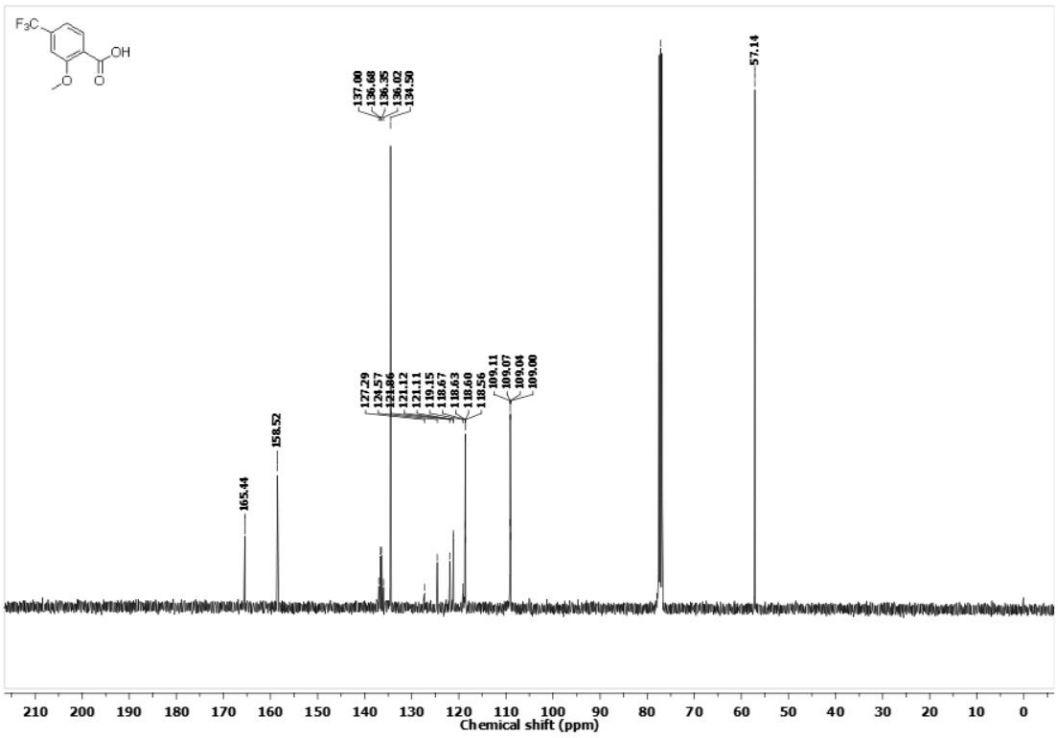

Figure 22: 101 MHz ^{13}C NMR spectrum of **6a** in $CDCl_3$. Solvent residual peak at 77.16 ppm.

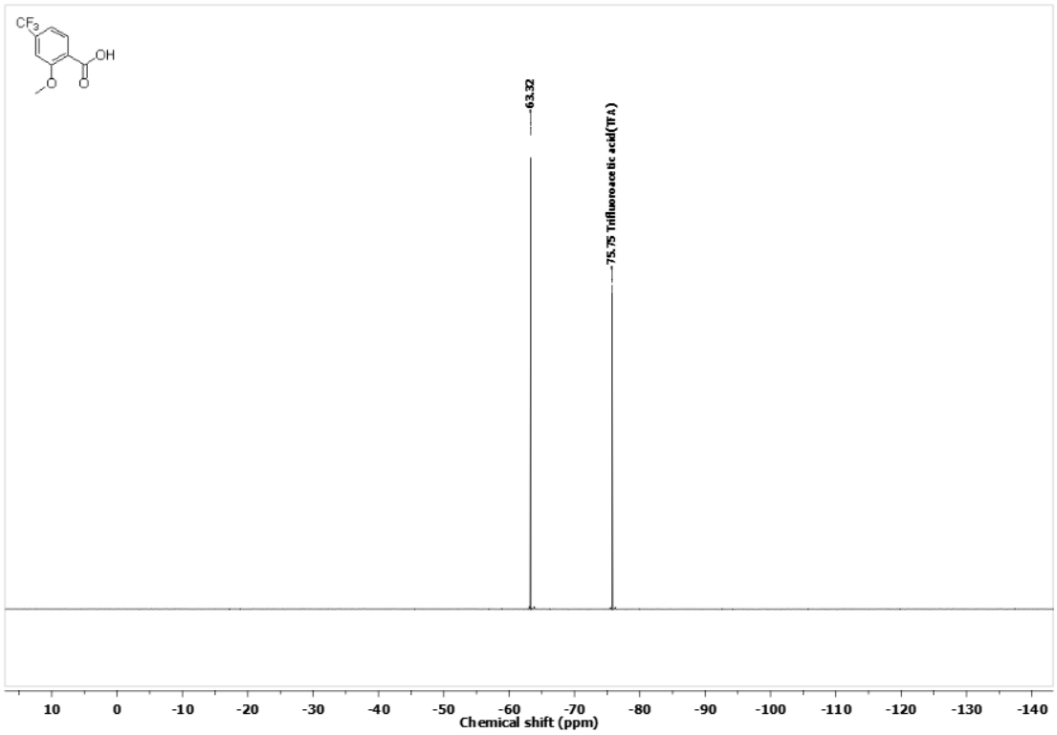

Figure 23: 377 MHz ^{19}F NMR spectrum of **6a** in $CDCl_3$. Internal reference peak at -75.75 ppm.

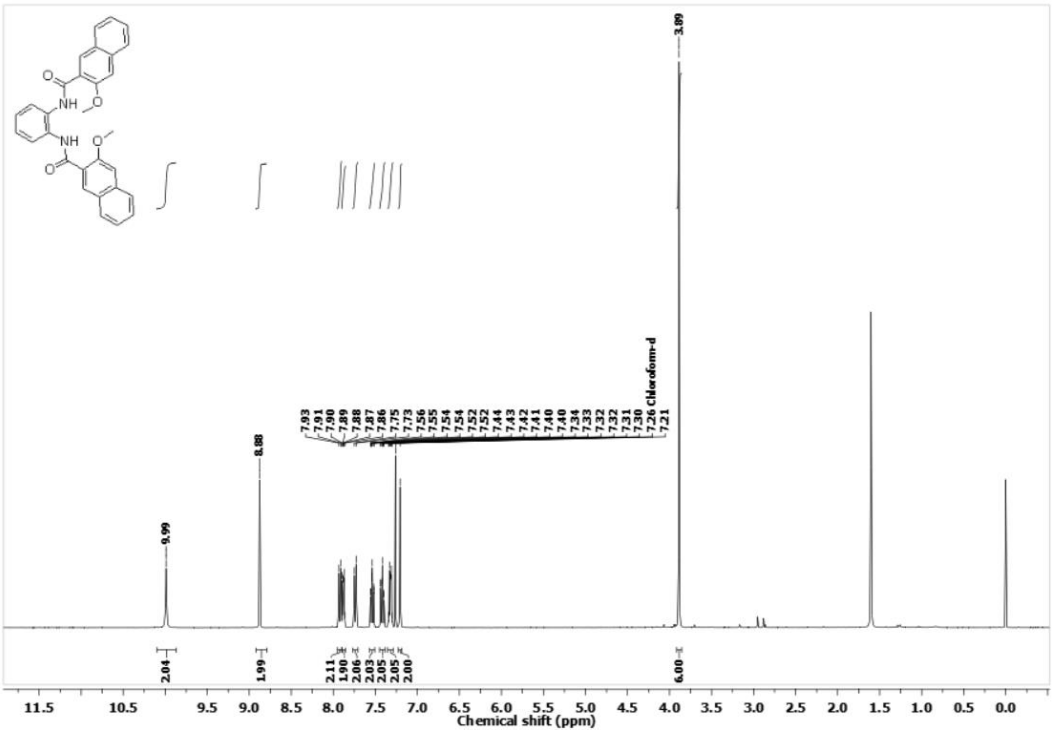

Figure 24: 400 MHz ^{1}H NMR spectrum of **5c** in $CDCl_3$. Solvent residual peak at 7.26 ppm.

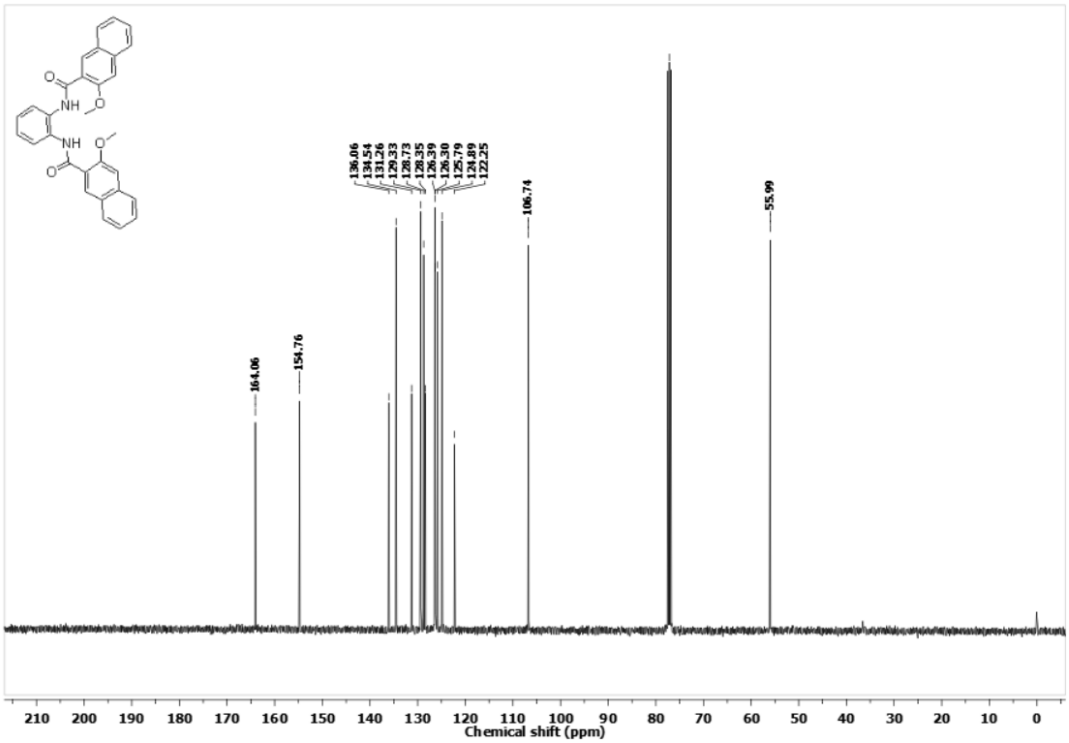

Figure 25: 101 MHz ^{13}C NMR spectrum of **5c** in $CDCl_3$. Solvent residual peak at 77.16 ppm.

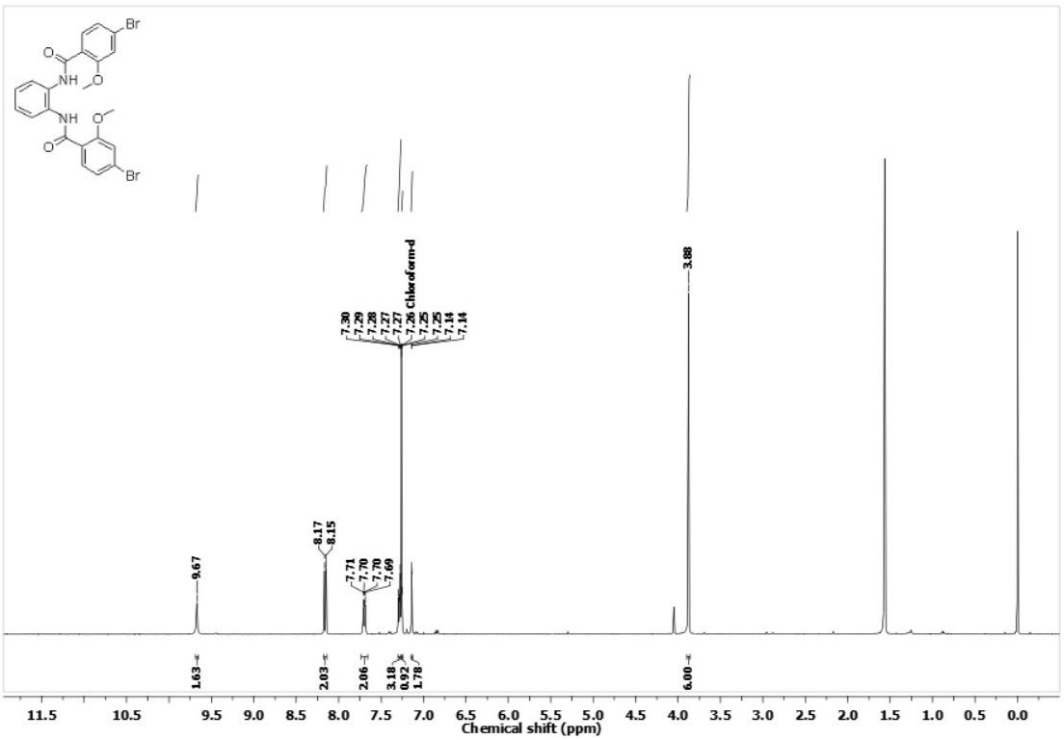

Figure 26: 400 MHz ^{1}H NMR spectrum of **5b** in $CDCl_3$. Solvent residual peak at 7.26 ppm.

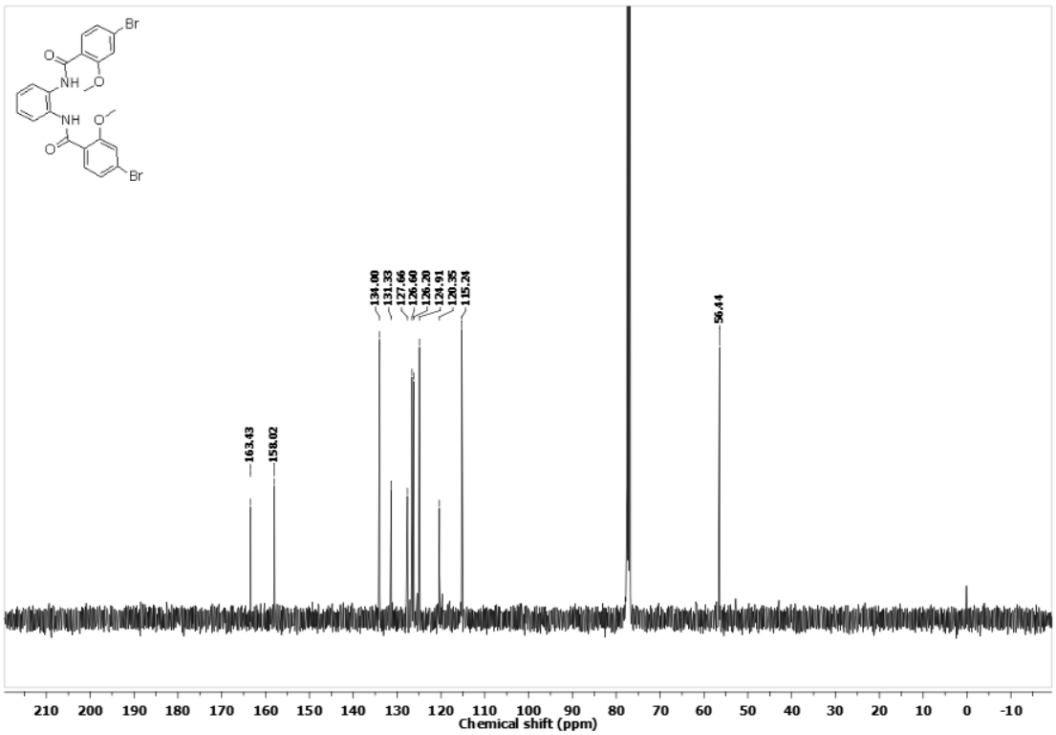

Figure 27: 101 MHz ^{13}C NMR spectrum of **5b** in $CDCl_3$. Solvent residual peak at 77.16 ppm.

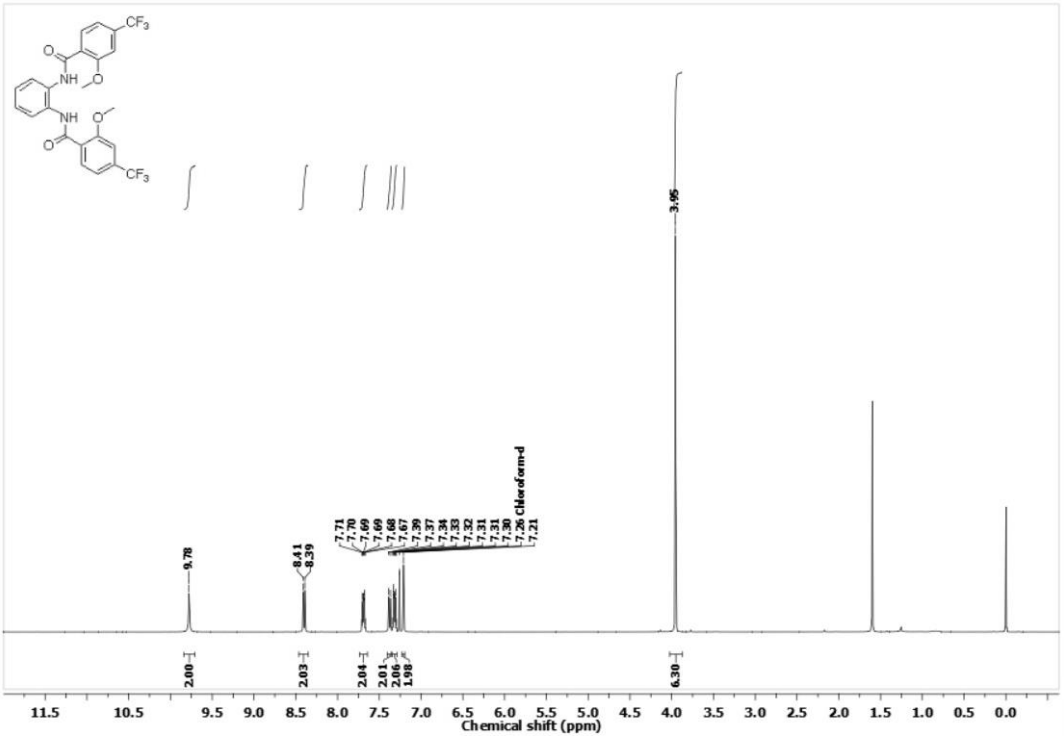

Figure 28: 400 MHz ^{1}H NMR spectrum of **5a** in $CDCl_3$. Solvent residual peak at 7.26 ppm.

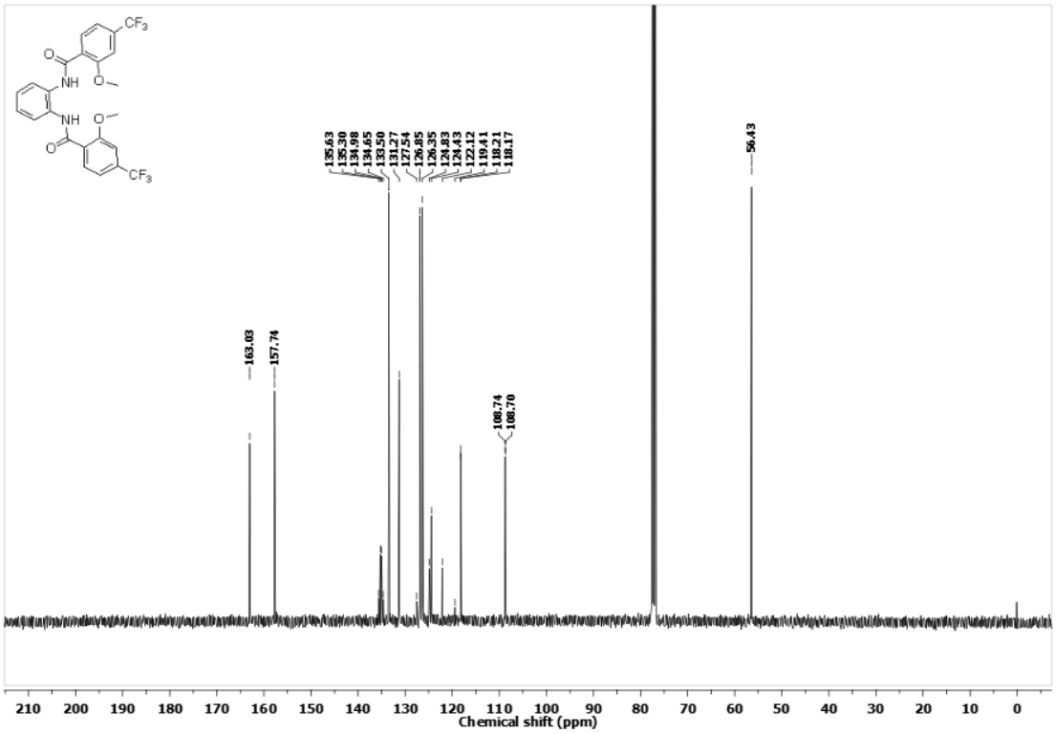

Figure 29: 101 MHz ^{13}C NMR spectrum of **5a** in $CDCl_3$. Solvent residual peak at 77.16 ppm.

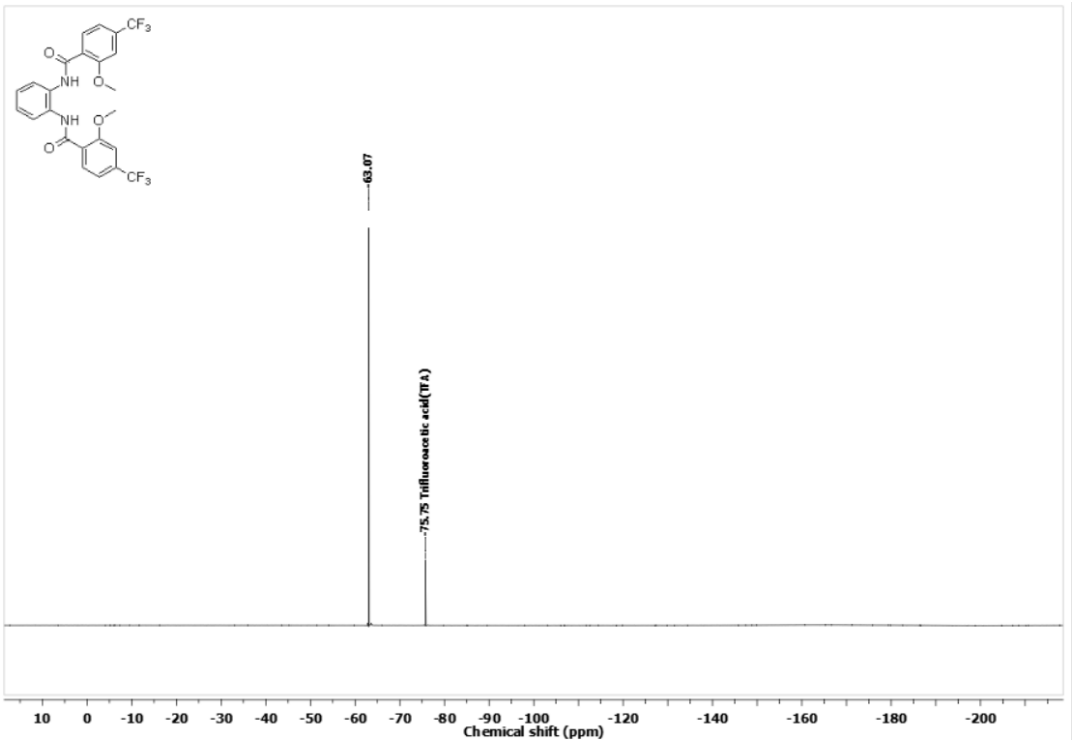

Figure 30: 377 MHz ^{19}F NMR spectrum of **5a** in $CDCl_3$. Internal reference peak at -75.75 ppm.

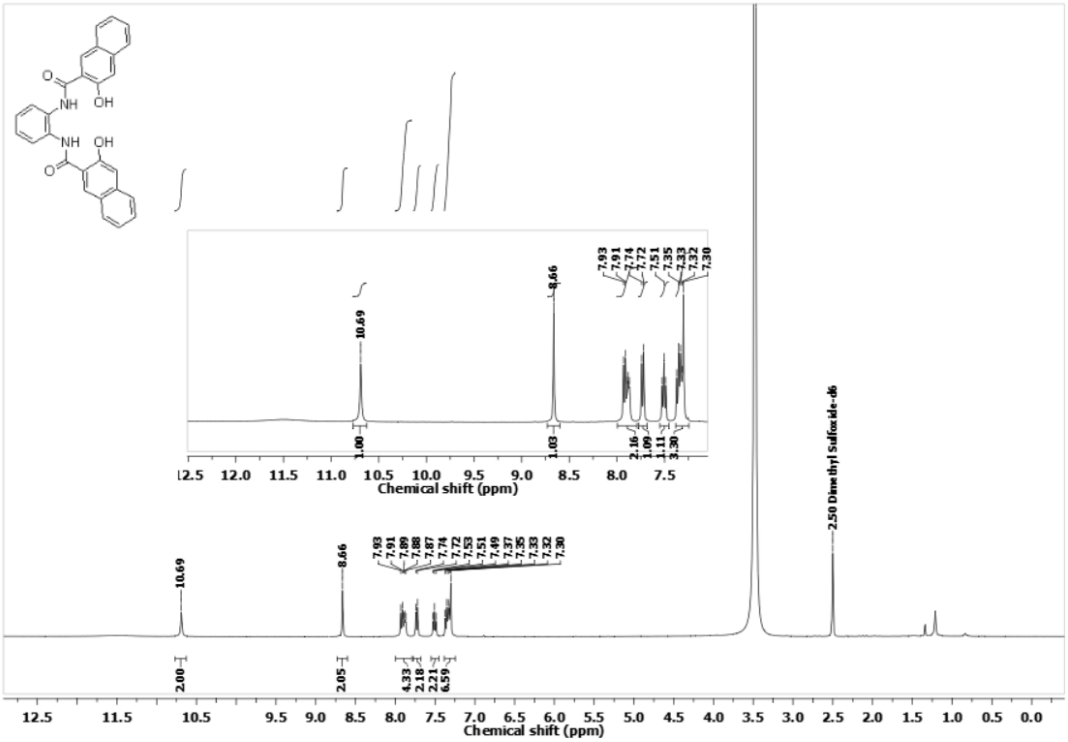

Figure 31: 400 MHz ^{1}H NMR spectrum of **2c** in DMSO-D_6. Solvent residual peak at 2.50 ppm.

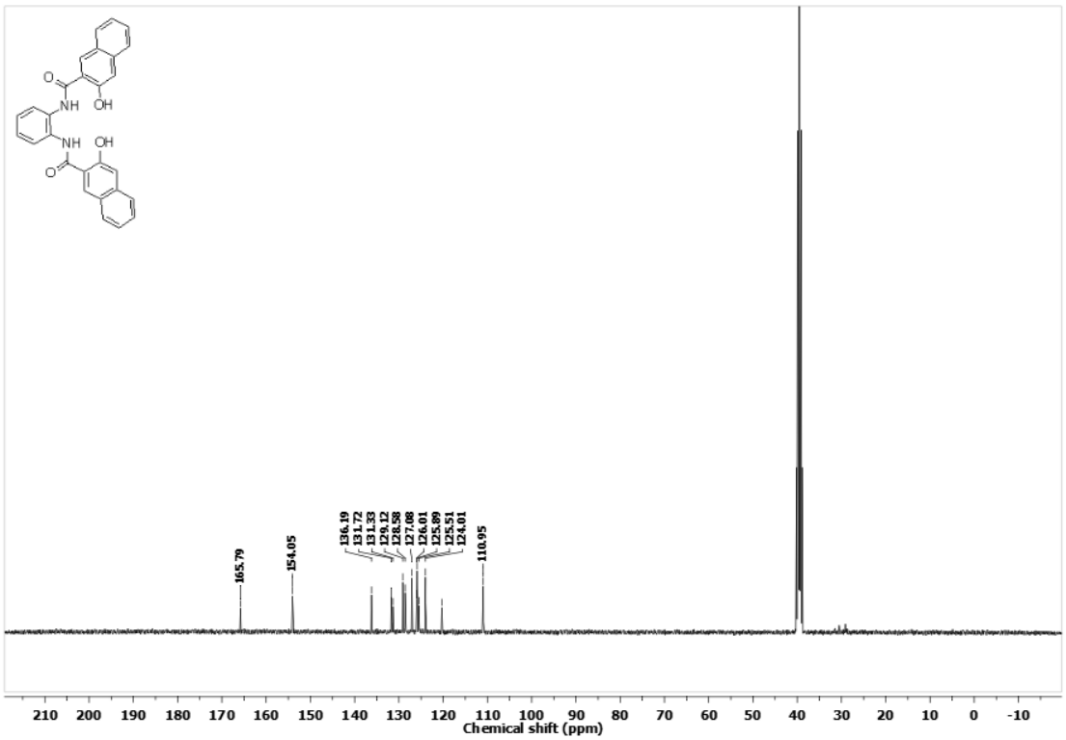

Figure 32: 101 MHz ^{13}C NMR of **2c** in DMSO-d_6.Solvent residual peak at 39.52 ppm.

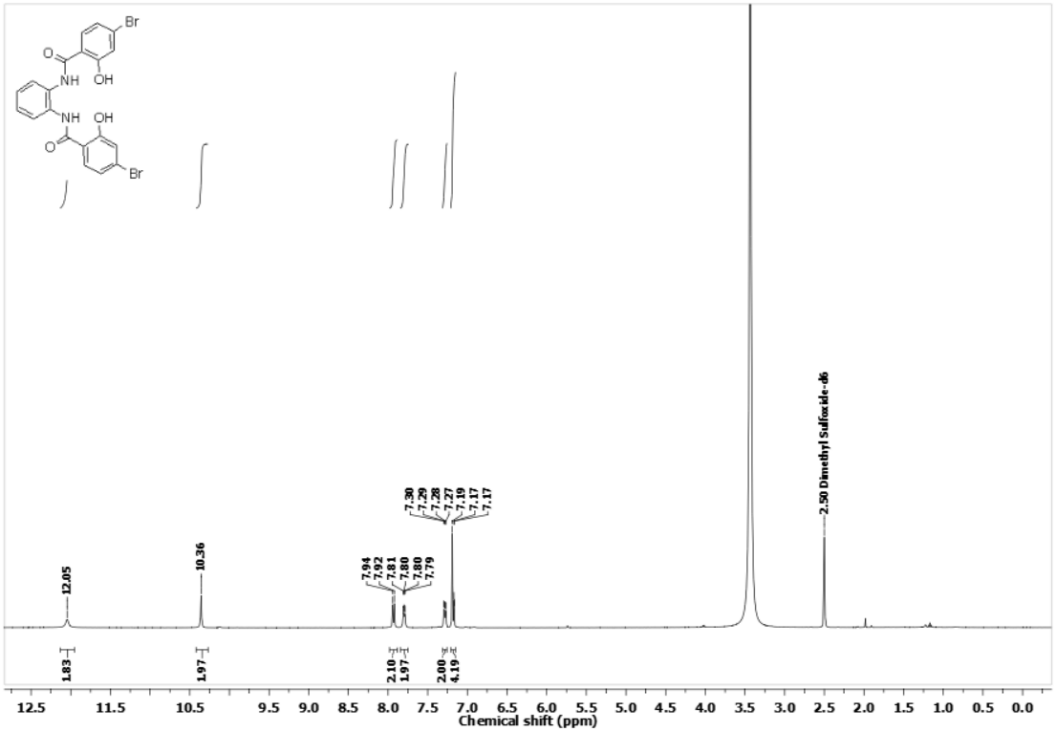

Figure 33: 400 MHz ^{1}H NMR spectrum of **2c** in DMSO- d_6. Solvent residual peak at 2.50 ppm.

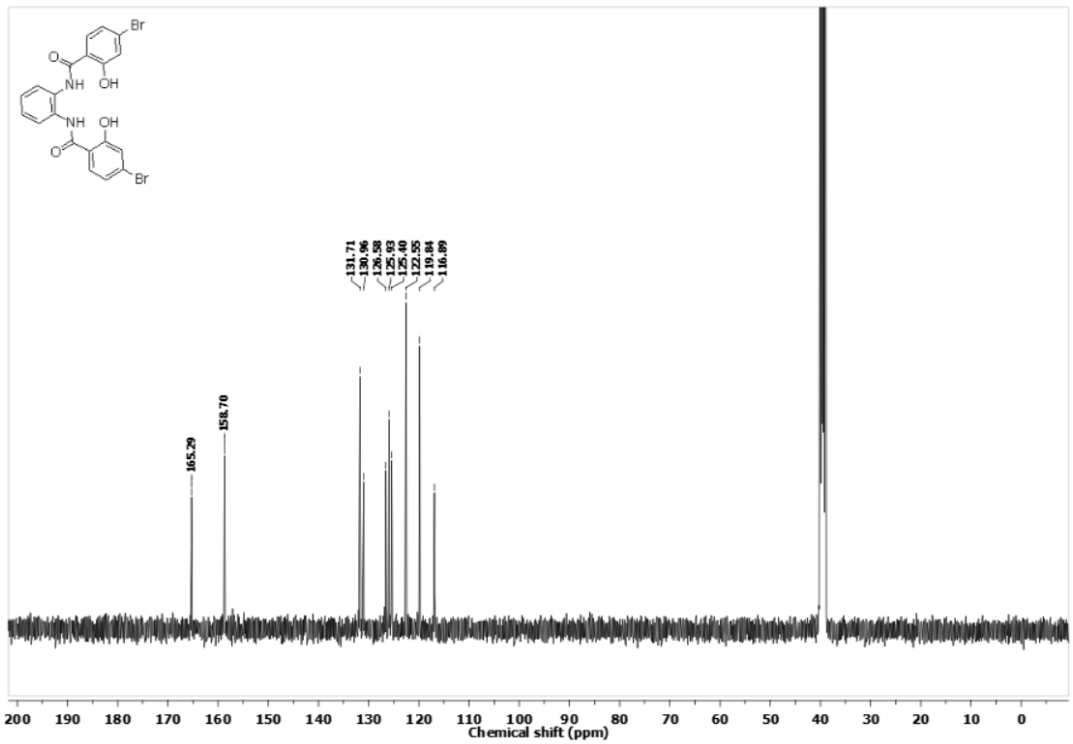

Figure 34: 101 MHz ^{13}C NMR of **2b** in DMSO- d_6.Solvent residual peak at 39.52 ppm.

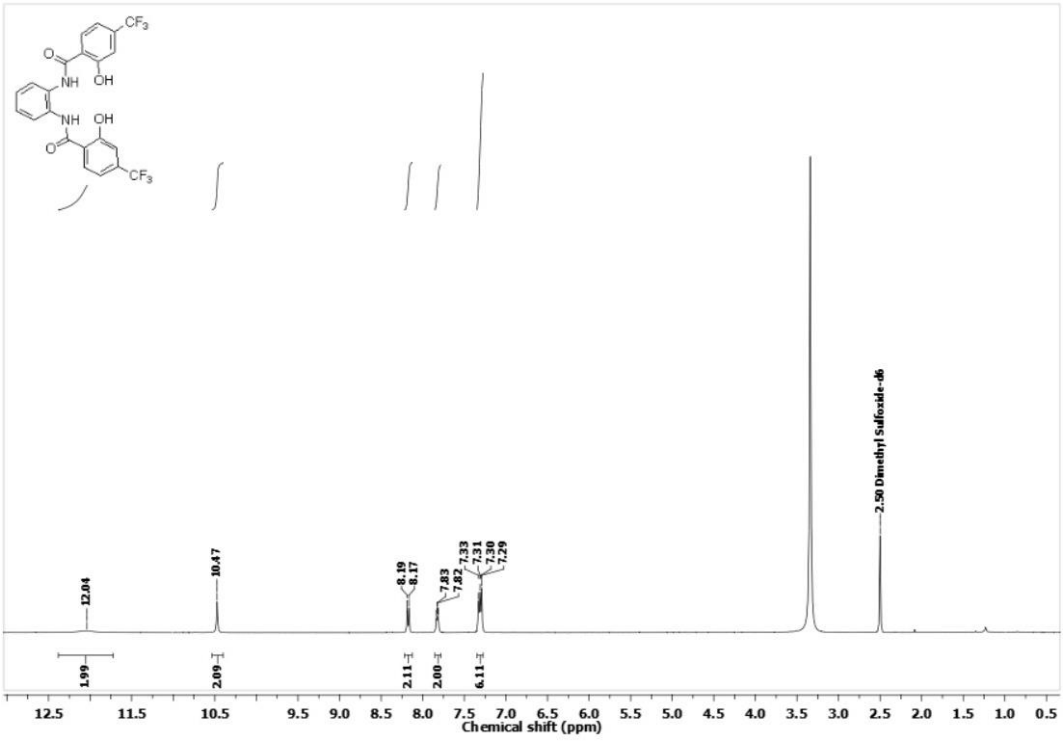

Figure 35: 400 MHz ^{1}H NMR spectrum of **2a** in DMSO- d_6. Solvent residual peak at 2.50 ppm.

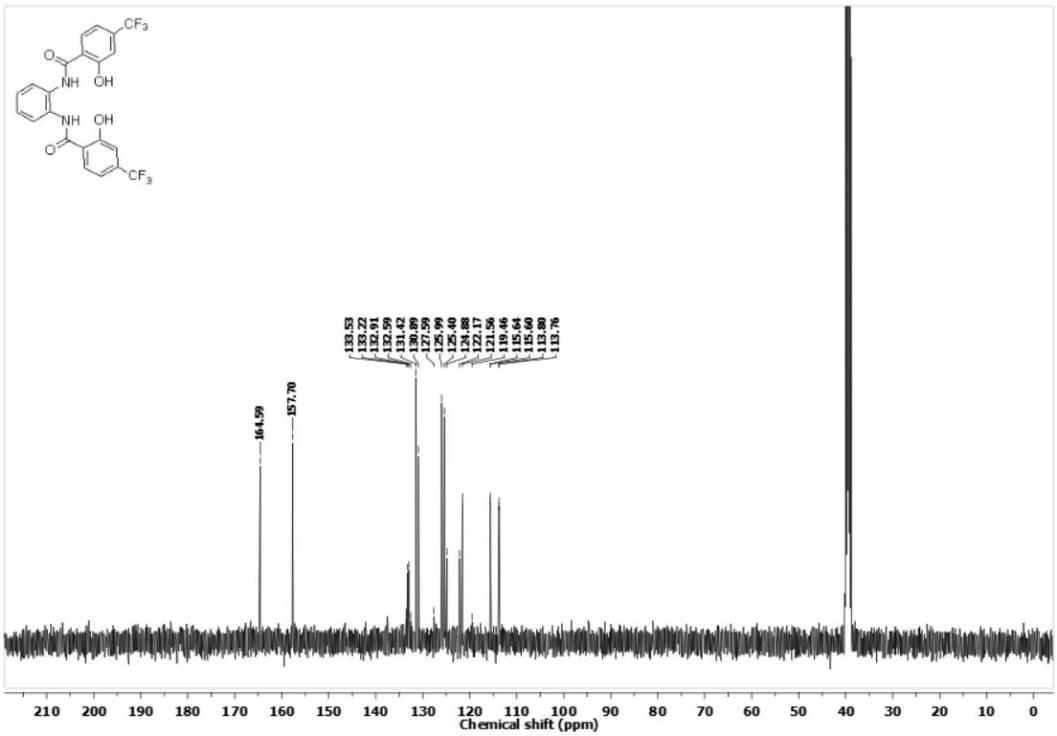

Figure 36: 101 MHz ^{13}C NMR of **2a** in DMSO- d_6.Solvent residual peak at 39.52 ppm.

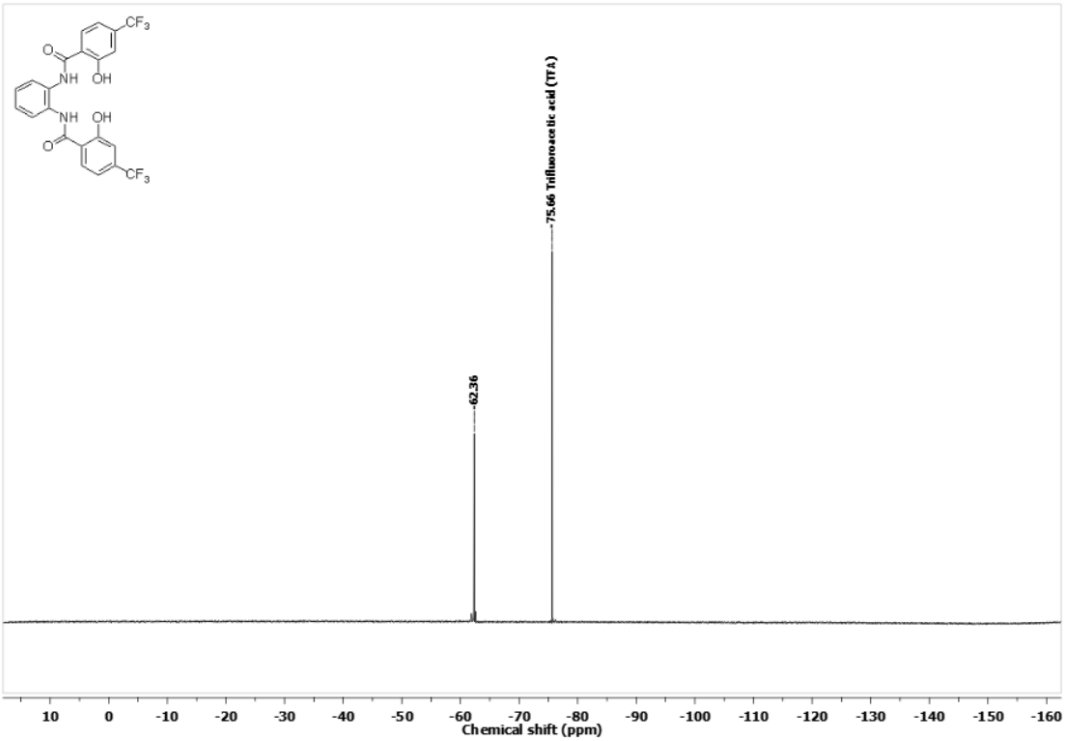

Figure 37: 377 MHz ^{19}F NMR of **2a** in DMSO-d_6. Solvent residual peak at 75.66 ppm.

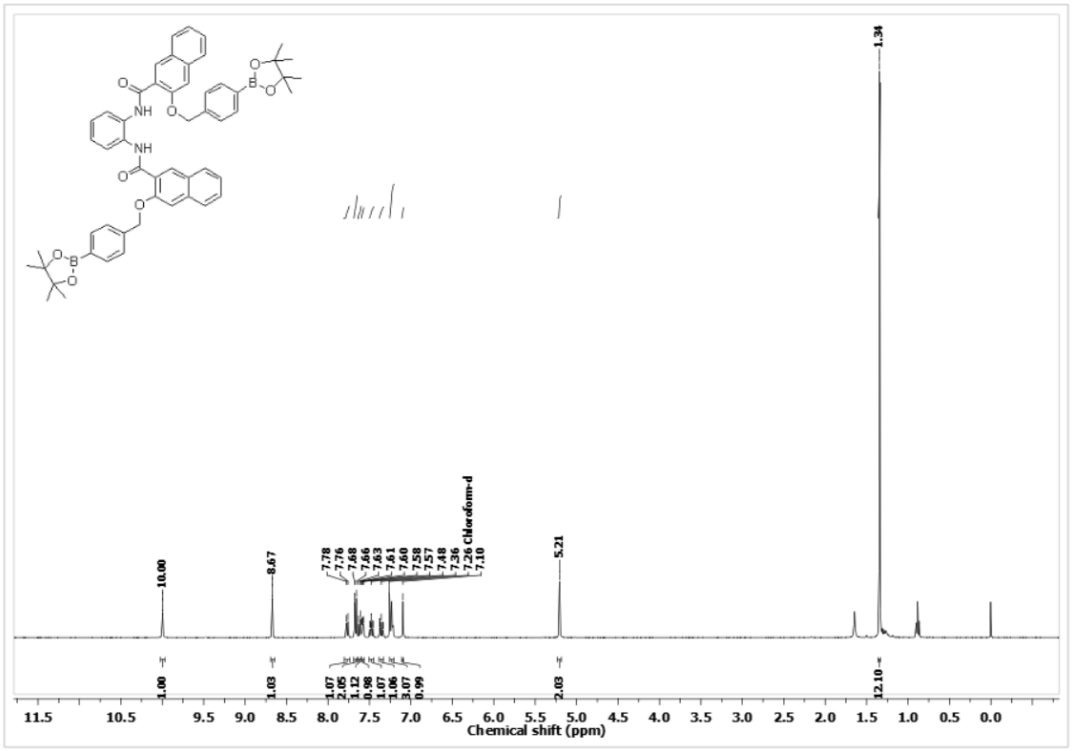

Figure 38: 400 MHz ^{1}H NMR spectrum of **1c** in DMSO- d_6. Solvent residual peak at 2.50 ppm.

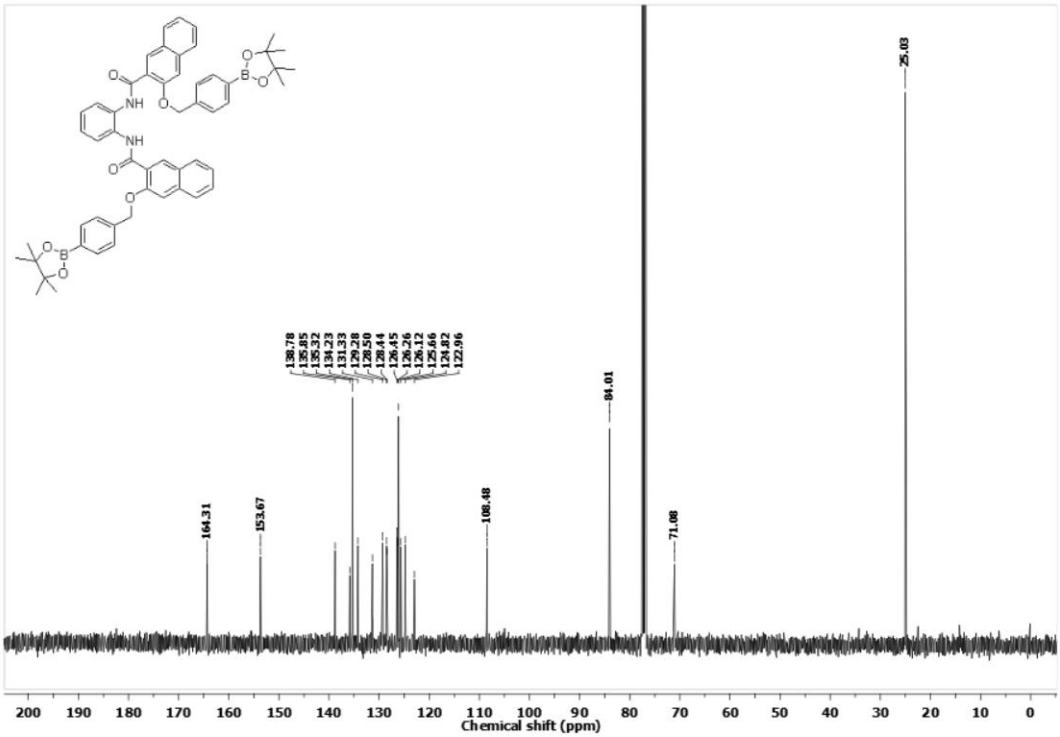

Figure 39: 101 MHz ^{13}C NMR of **1c** in DMSO- d_6.Solvent residual peak at 39.52 ppm.

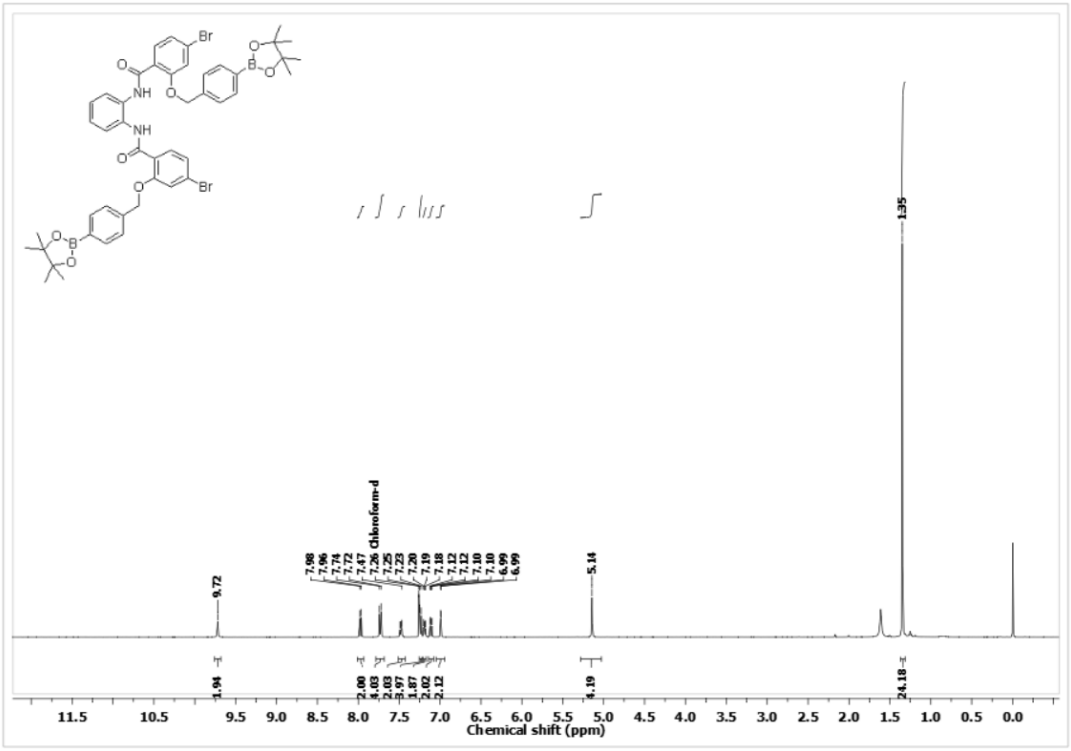

Figure 40: 400 MHz ^{1}H NMR spectrum of **1c** in DMSO- d_6. Solvent residual peak is 2.50 ppm.

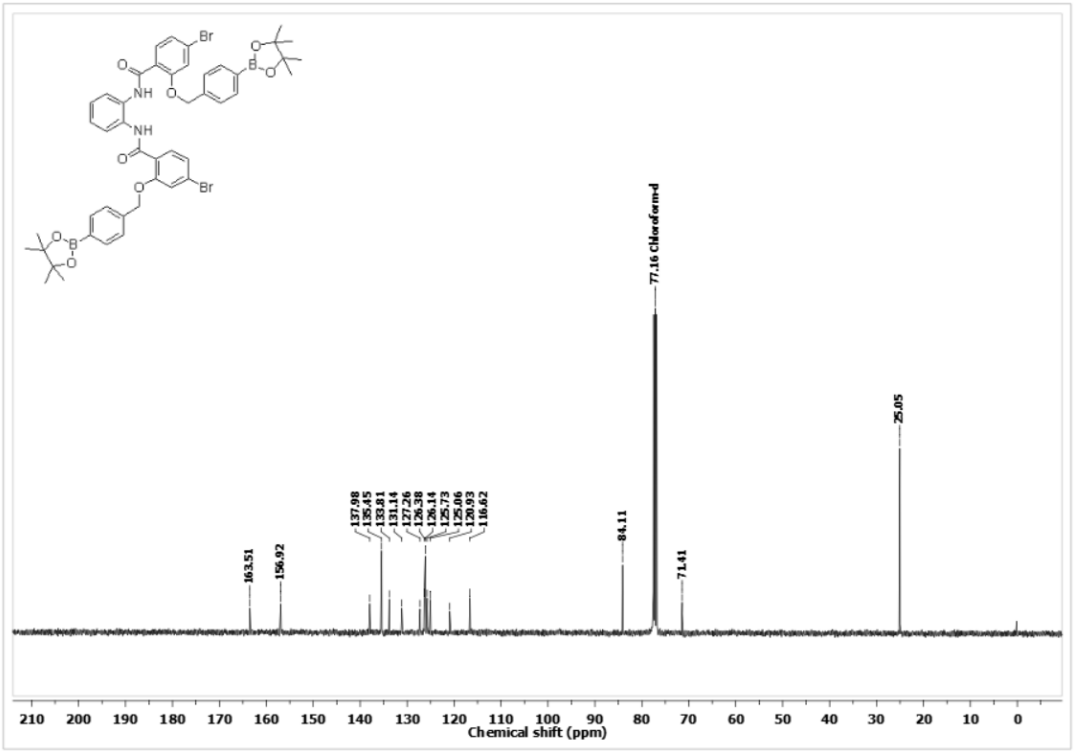

Figure 41: 101 MHz ^{13}C NMR of **1b** in DMSO- d_6. Solvent residual peak at 39.52 ppm.

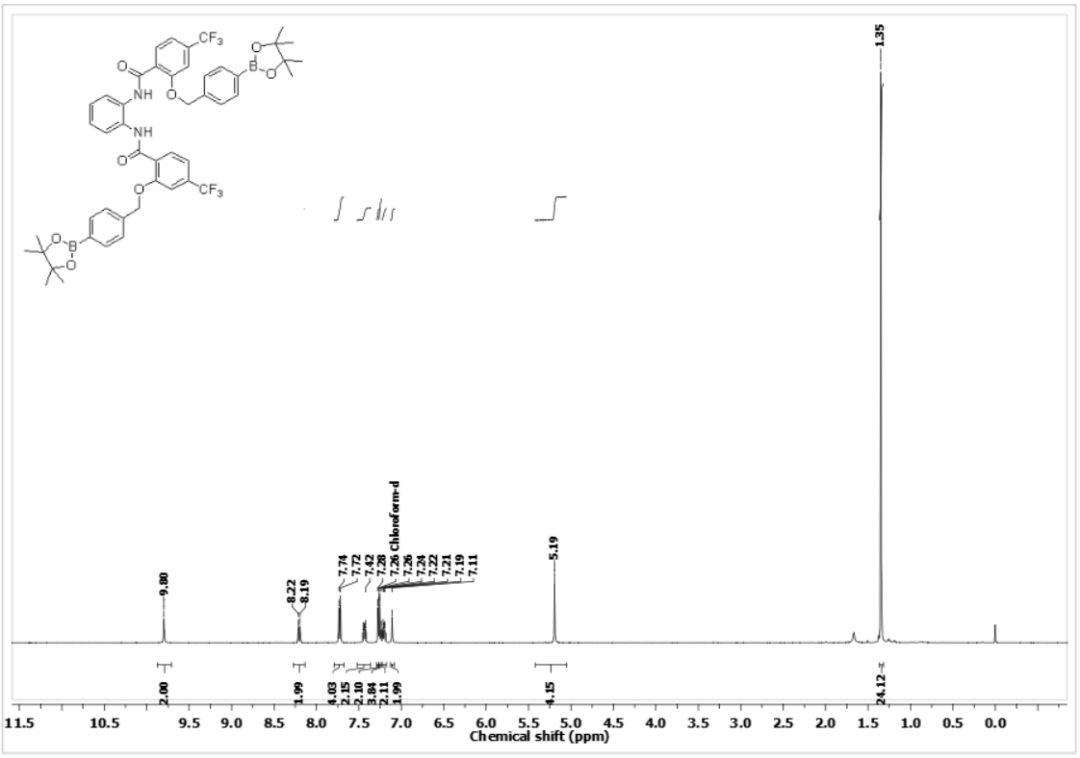

Figure 42: 400 MHz ^{1}H NMR spectrum of **1a** in DMSO- d_6. Solvent residual peak at 2.50 ppm.

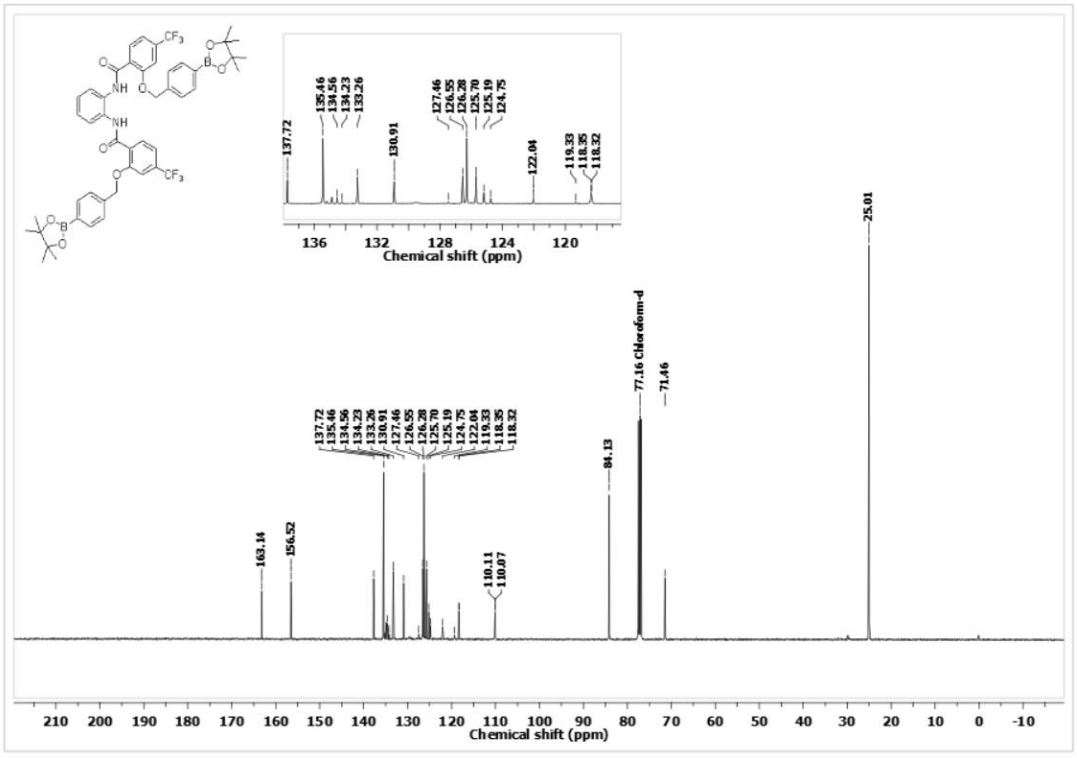

Figure 43: 101 MHz ^{13}C NMR of **1a** in DMSO- d_6. Solvent residual peak at 39.52 ppm.

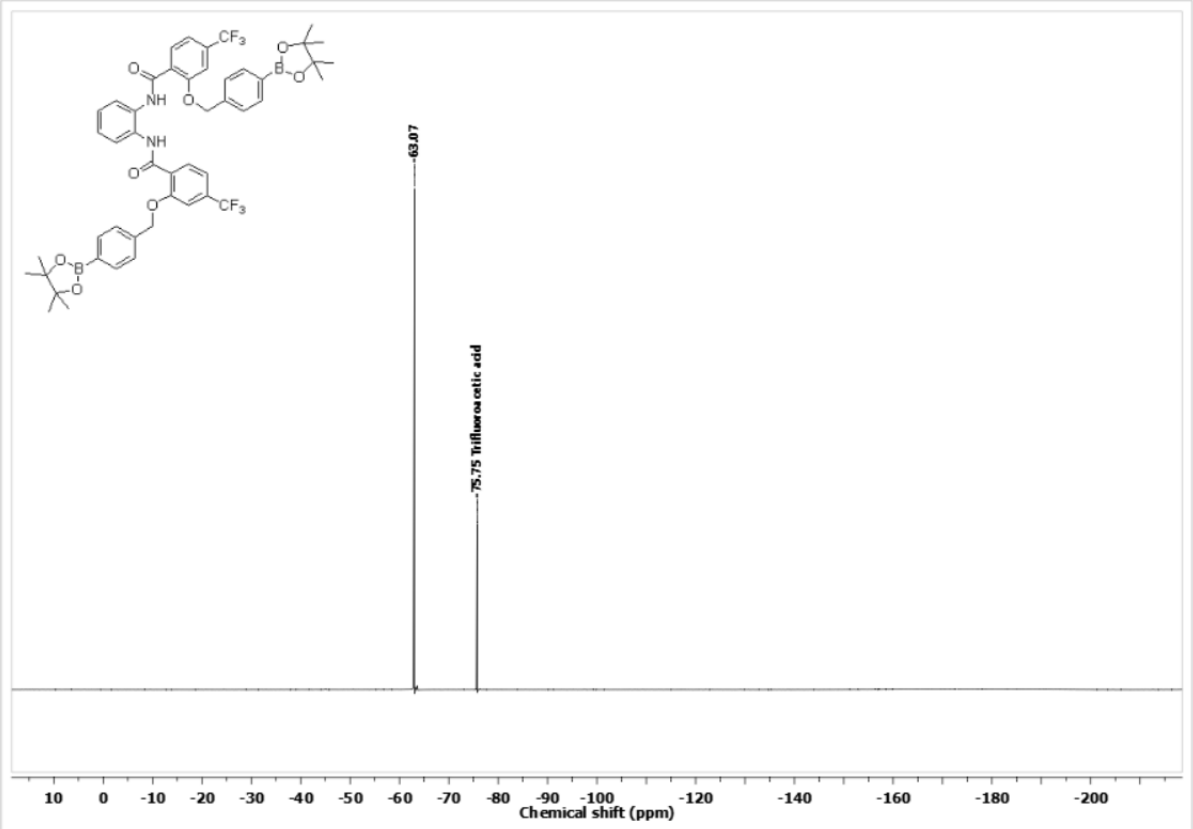

Figure 44: 377 MHz ^{19}F NMR of **1a** in DMSO-d_6. Solvent residual peak at 75.66 ppm.

6. Conclusion

We have successfully synthesized and characterised three derivatives of the transporter and protransporter. Further the activation of protransporter to transporter was confirmed using TLC, MALDI and HRMS techniques. At the same time regeneration of the transport activity was evaluated using lucigenin assay and the results were found to be satisfactory. Finally after the confirmation of ion transporter regeneration and regain of ion transport in model system, the protransporters(Br and Napthyl derivative) were found to be harmless to the cancer cells while the transporter(**2b**) was harmful for the cell. Optimization for the activation is still under process at the time of this writing.

7. References

1. Kim, J.-B., Channelopathies. *Korean J. Pediatr.* **2014,** *57*, 1-18.
2. Gale, P. A.; Davis, J. T.; Quesada, R., Anion transport and supramolecular medicinal chemistry. *Chem. Soc. Rev.* **2017,** *46*, 2497-2519.
3. Saha, T.; Hossain, M. S.; Saha, D.; Lahiri, M.; Talukdar, P., Chloride-Mediated Apoptosis-Inducing Activity of Bis(sulfonamide) Anionophores. *J. Am. Chem. Soc.* **2016,** *138*, 7558-7567.
4. Akhtar, N.; Pradhan, N.; Saha, A.; Kumar, V.; Biswas, O.; Dey, S.; Shah, M.; Kumar, S.; Manna, D., Tuning the solubility of ionophores: glutathione-mediated transport of chloride ions across hydrophobic membranes. *Chem. Commun.* **2019,** *55*, 8482-8485.
5. Wu, Y.; Guo, T.; Qiu, Y.; Lin, Y.; Yao, Y.; Lian, W.; Lin, L.; Song, J.; Yang, H., An inorganic prodrug, tellurium nanowires with enhanced ROS generation and GSH depletion for selective cancer therapy. *Chem. Sci.* **2019,** *10*, 7068-7075.
6. Szatrowski, T. P.; Nathan, C. F., Production of Large Amounts of Hydrogen Peroxide by Human Tumor Cells1. *Cancer Res.* **1991,** *51*, 794-798.
7. Lippert, A. R.; Van de Bittner, G. C.; Chang, C. J., Boronate Oxidation as a Bioorthogonal Reaction Approach for Studying the Chemistry of Hydrogen Peroxide in Living Systems. *Acc. Chem. Res.* **2011,** *44*, 793-804.
8. Quin, C.; Robertson, L.; McQuaker, S.; Price, N.; Brand, M.; Hartley, R., Caged mitochondrial uncouplers that are released in response to hydrogen peroxide. *Tetrahedron* **2010,** *66*, 2384-2389.
9. Busschaert, N.; Park, S.-H.; Baek, K.-H.; Choi, Y. P.; Park, J.; Howe, E. N. W.; Hiscock, J. R.; Karagiannidis, L. E.; Marques, I.; Félix, V.; Namkung, W.; Sessler, J. L.; Gale, P. A.; Shin, I., A synthetic ion transporter that disrupts autophagy and induces apoptosis by perturbing cellular chloride concentrations. *Nat. Chem.* **2017,** *9*, 667-675.
10. Legg, K. D.; Hercules, D. M., Quenching of lucigenin fluorescence. *J. Phys. Chem.* **1970,** *74*, 2114-2118.
11. Kuete, V.; Karaosmanoğlu, O.; Sivas, H., Chapter 10 - Anticancer Activities of African Medicinal Spices and Vegetables. In *Medicinal Spices and Vegetables from Africa*, Kuete, V., Ed. Academic Press: 2017; pp 271-297.
12. Kamiloglu, S.; Sari, G.; Ozdal, T.; Capanoglu, E., Guidelines for cell viability assays. *Food Front.* **2020,** *1*, 332-349.
13. https://microbenotes.com/vesicles-structure-types-and-functions/